TECHNISCHE UNIVERSITÄT MÜNCHEN

Fakultät für Medizin

The role of distinct microRNAs in stemness and malignancy of Ewing sarcoma and their epigenetic regulation

Esther Franziska Heid

Vollständiger Abdruck der von der Fakultät für Medizin der Technischen Universität München zur Erlangung des akademischen Grades eines Doktors der Medizin genehmigten Dissertation.

Vorsitzender: Prof. Dr. Jürgen Schlegel

Prüfer der Dissertation:

1. Priv. - Doz. Dr. Günther Richter
2. Prof. Dr. Stefan Burdach

Die Dissertation wurde am 13.03.2017 bei der Technischen Universität München eingereicht und durch die Fakultät für Medizin am 03.01.2018 angenommen.

Table of Contents

List of abbreviations

6BL1	Abelson murine leukemia viral oncogene homolog 1
AGO	Agonaute protein
BCL-2	B-cell lymphoma 2
BRCA1	breast Cancer 1
BrdU	Bromodeoxyuridine
BRD	Bromodomain containing proteins
BET	bromo and extraterminal protein
cALL	common acute lymphoblasic leukemia
cDNA	complementary DNA
ChIP	Chromatin immunoprecipitation
DGCR8	DiGeorge syndrome critical region gene 8
DMSO	Dimetylsulfoxide
DNA	desoxyribonucleic acid
DNMT	DNA methyltransferase
EDTA	Ethane-1,2-diyldinitrilo tetraacetic acid
EED	embryonic ectoderm development
ERG	v-ets avian erythroblastosis virus E26 oncogene homolog
ES	Ewing sarcoma
ESFT	Ewing sarcoma family of tumors
ETS	e-twenty six transcription factor (leukemia virus E26)
EWS	Ewing sarcoma breakpoint region 1
EZH2	enhancer of zeste (Drosophila) homolog 2
FACS	fluorescence activated cell sorting
FBS	fetal bovine serum
FLI1	friend leukemia integration 1
GAPDH	Glyceraldehyde 3-phosphate dehydrogenase

H3	histone 3
H3K27me3	histone 3 lysine 27 trimethylation
HAT	Histone acetyltransferases
HDAC	Histone deacetylase
H&E	Hematoxylin & Eosin
IGF	insulin-like growth factor
miRNA	microRNA
mRNA	messenger RNA
MSC	mesenchymal stem cell
NANOG	nanog homeobox
PBS	phosphate buffered saline
PCR	polymerase chain reaction
PACT	protein activator of protein kinase R
PAS	periodic acid Schiff
PcG	polycomb group
pPNET	peripheral primitive neuroectodermal tumor
PRC 2	polycomb repressive complex 2
pRT-PCR	quantitative real time PCR
RISC	RNA-induced silencing complex
RLC	RISC loading complex
RNA	ribonucleic acid
RNAi	RNA interference
SDS	sodium dodecyl sulfate
shRNA	small hairpin RNA
siRNA	short interfering RNA
snoRNA	small-nucleolar RNA
SOX 2	sry-box 2
SUZ 12	scaffold protein suppressor of Zeste
TBST	Tris-Buffered Saline Tween-20
TEMED	N,N,N',N'-Tetramethylethan-1,2-diamin

TRBP	RISC-loading complex subunit
TSA	Trichostatin A
UTR	untranslated region
5-AzaC	5-Aza-Cytidine

1. Introduction

1.1 The Ewing sarcoma

Ever since the American pathologist James Ewing has first described *a diffuse endothelioma of the bone* (Ewing, 1972) in 1921, its unclear histopathological origin has bothered many scientist and has not yet been understood completely. Ewing sarcoma (ES) is the second most common bone cancer in childhood and young adolescence following the osteosarcoma. It occurs with an approximate incidence of 5 per million and has a peak occurrence around the age of 15 years (Kaatsch & Spix, 2015). The median age at diagnosis is 10 years and 11 month whereas marginally more males than females and more Caucasians are affected (Bernstein et al., 2006). Usually the first symptom is local pain that can easily be mistaken as “bone growth” or an injury resulting from sportive activities. Primarily, because the majority of patients is in its second decade of life and thus very active. With proceeding tumor growth and initiating metastasis the disease attracts immediate attention. Thereby, especially tumor bulk, local pain and other unspecific symptoms such as fever and malaise plead for a malignant process.

The most common primary tumor sides are the long bones of the lower extremities, the pelvis, the axial skeleton and the ribs, whereas the tumor characteristically arises from the diaphysis (Bernstein et al., 2006). Besides the frequent manifestation in bone tissue, 15% of ES is found even extra-osseous, most likely in soft tissue parts of the body (Riggi, Suvà, & Stamenkovic, 2009). Patients with local disease already benefit from modern multimodal therapeutic regimens including chemotherapy, surgery and radiotherapy (Burdach & Jürgens, 2002; Lahl, Fisher, & Laschinger, 2008) that improved the five year survival up to 70%. Nevertheless, those 25% with metastasis at the moment of diagnosis still have poor outcome. Primary metastasis is detectable in lung and bone tissue, whereas especially bone metastasis reduces the five year survival to less than 10% (Bernstein et al., 2006).

The most common type of ES is part of a family of different tumors that share similar histologic appearance as well as molecular and immunohistochemical features (Pinto, Dickman, & Parham, 2011). Apart from the classical ES, the *Ewing sarcoma family of tumors* (ESFT) consists of the *peripheral neuroepithelioma*, the *peripheral primitive neuroectodermal tumor* (pPNET) and the *Askin tumor*. Even though ES cells show

mesenchymal, neuroectodermal as well as endothelial properties (Staege et al., 2004) the precise cell of origin is still unknown.

The histologic feature is monomorphic and undifferentiated. It displays round small blue cells after *hematoxylin* and *eosin* (H&E) staining and a positive response after *periodic acid Schiff reaction* (PAS). Moreover, there is just little mitosis activity (Böcker & Aguzzi, 2008). However, the described morphology is not characteristic for ES. There are some other pediatric tumors such as neuroblastoma and leukemia that make it difficult to distinguish. For that reason it is necessary to examine more specific features. ES shows a strong expression of several immunohistochemical markers, including the membrane associated protein CD99, friend leukemia virus integration 1 (FLI1) and caveolin (Pinto et al., 2011). Additionally, ES has a characteristic genetic background that is a balanced chromosomal translocation between chromosomes 11 and 22, which leads to an aberrant oncogene. This gene arrangement includes the N-terminal transcriptional regulatory domain of the *EWS* gene (*Ewing sarcoma breakpoint region 1*) from chromosome 22q12 and one gene of the *ETS* family (*e-twenty-six*) that encodes for transcription factors. In 85% of all cases this *ETS* gene is represented by the DNA-binding domain of *FLI1* (chromosome 11q24), followed by the *ERG* gene (*v-ets avian erythroblastosis virus E26 oncogene homolog*) in about 10% of cases (Burchill, 2003; Jedlicka, 2010). The product of this translocation *EWS/FLI1* yields a strongly expressed and potent transcription factor that works as a transcriptional activator as well as a repressor. Hence it influences gene expression and oncogenic transformation (Sankar et al., 2013).

Recent studies tried to gain a better understanding of EWS/FLI1 and its influence on multiple oncogenic hits. Therefore, EWS/FLI1 knock down was performed by RNA interference in patient-derived ES cell lines. Treated cells displayed a gene-expression pattern that was similar to those of mesenchymal stem cells (MSC). These cells were able to differentiate into different mesodermal cell lines such as chondrocytes or osteoblasts (Feng & Chen, 2009; Lessnick & Ladanyi, 2012; Tirode et al., 2007). In addition, the inhibition of EWS/FLI1 in ES cells allowed the differentiation into those differentiated cells as well.

Other experiments started with MSCs and the introduction of EWS/FLI1, whereas it was possible to induce oncogenic transformation (Riggi et al., 2005). These results suggested that MSC could be the cell of origin of ES.

Apparently, EWS/FLI1 is able to influence other genes and mechanisms that contribute to the oncogenic transformation and are important for proliferation and differentiation. After the introduction of EWS/FLI1 into MSCs the fusion protein induced the expression of different embryonic stem cell genes such as *NANOG* or *SOX2*, which are able to reprogram differentiated cells (Riggi et al., 2010). Additionally, EWS/FLI1 increases the expression of the histone methyltransferase enhancer of zeste (Drosophila) homolog 2 (EZH2), which is an enzyme of histone modification (Richter et al., 2009).

Nevertheless, the exact mechanisms how EWS/FLI1 regulates target genes have not been understood completely. Therefore, Riggi et al. examined direct chromatin remodeling events influenced by EWS/FLI1. At first, they discovered GGAA repeats in the DNA sequence of regulatory elements that are bound by EWS/FLI1 to promote histone acetylation and thus gene activation. In a second step, they were able to demonstrate that EWS/FLI1 represses existing enhancers by displacing endogenous ETS activators from their binding sites (Riggi et al., 2014).

Even microRNAs (miRNAs) revealed to be influenced by EWS/FLI1. Ban et al. discovered miR-145 to depend on EWS/FLI1 and vice versa. Artificial up-regulation of miR-145 reduced EWS/FLI1 expression and altered the ES cell proliferation capacity (Ban et al., 2011).

Characteristically, oncofusion gene-driven tumors like ES indicate a low mutation rate. However, ES has been reported to contain a low number of relevant mutations in coding regions (Lawrence et al., 2013). Accordingly, Agelopoulos et al. used ES tumor samples of 116 patients and performed whole genome sequencing (WGS) to identify potential drivers and relapse-associated genes. They discovered, that relapsed tumors show a 2- to 3-fold increased number of somatic mutations. Furthermore, they were able to identify mutations as well as a copy number gain of the *fibroblast growth factor receptor 1* gene (FGFR1) that resulted in an enhanced tyrosine kinase activity. ShRNA mediated knock down of FGFR1 reduced proliferation capacity *in vitro* and *in vivo* (Agelopoulos et al., 2015). This discovery provides evidence that besides EWS/FLI1, mutations of other genes (in this case *FGFR1)* contribute to the malignant phenotype of ES.

Since the survival rate of patients with metastatic spread, especially after the formation of bone metastases, is still fatal, there is an urgent requirement to get more information about the underlying molecular mechanisms of this tumor in order to develop new

therapeutic treatment strategies. Therefore, miRNAs seem to be an interesting candidate for possible future targeted therapies.

1.2 Epigenetics and gene regulation

The term “epigenetics” describes possible mechanisms of alterations in gene expression that do not depend on direct modification of the DNA. Epigenetic processes affect changes of the chromatin structure by modifying DNA packaging proteins and indirect DNA alterations by methylation. These modifications present dynamic regulators of gene activity and are important for nuclear architecture. There are three categories of proteins taking part in epigenetic regulation processes. The first category consists of writing enzymes that catalyze histone or DNA modifications such as histone and DNA methyltransferases. The second group of enzymes are so called erasers, enzymes that remove histone or DNA modifications including for example histone and DNA demethylases. Finally, the last category includes reading proteins that recognize a specific histone or DNA modification and modulate transcription by binding to these modifications (Shu & Polyak, 2017).

Histone modifications together with DNA methylation are involved in the regulation of protein biosynthesis and even in DNA repair mechanisms (Egger, Liang, Aparicio, & Jones, 2004). Hence, alterations in epigenetics play an important role in cancer development and thus need to be examined.

1.2.1 DNA modification

The by now best investigated epigenetic modification process is the methylation of certain cytosins that are followed by guanines. These so called CpG islands arise mainly in the 5’ regulatory end region of many genes and include the promotor, the untranslated region as well as the first Exon. The methylation is carried out by an enzyme called DNA methyltranferase (DNMT) and hypermethylation of CpGs leads to gene silencing as it disrupts transcription (Herman & Baylin, 2003). Usually, CpG islands are not methylated in normal cells, however, methylation of particular subgroups of promoter CpG islands can be found even in normal tissue. Genomic imprinted genes are one example where DNA methylation at one of the two parental alleles of a gene ensures monoallelic expression.

Epigenetic processes normally influence each other and so DNA methylation appears even in the context of chemical modifications of histone proteins. Hypermethylated CpG islands are often associated with deacetylation of H3 and H4 (Fahrner, Eguchi, Herman, & Baylin, 2002). Therefore a number of proteins involved in DNA methylation directly interact with histone-modifying enzymes (Dobosy & Selker, 2001; Esteller, 2007).

1.2.2 Histone modification

DNA is reeled up with the help of histones. The resulting structural units are called nucleosomes. There exist five major families of histones: H1, H2A, H2B, H3 and H4 whereas histones H2A, H2B, H3 and H4 are known as the core histones, histone H1 is employed to stabilize the DNA. Amino acids of the N-terminal tail domain of the four core histones can be modified by different chemical post-transcriptional modification steps such as acetylation or methylation (Turner, 2002). Thus, methyl, phosphate and acetyl groups can be attached to Lysine, Arginine and Serine residues. Furthermore, this reactions can be repeated resulting in a rise of the degree of methylation / acetylation. Generally, acetylation is accompanied by gene activation. Therefore, histone acetyltransferases (HATs) catalyze a reaction in which the acetyl group neutralizes the positive charged amino acid of the histone. As a result the affinity of binding between the histone and the negative charged DNA decreases and thus forges active euchromatin which allows transcriptional procedures. However, there are also histone deacetylases (HDACs) that remove acetyl groups and accordingly arrange gene inactivation by forming inaccessible heterochromatin (Jenuwein & Allis, 2001; Schübeler et al., 2004).

In contrast to DNA methylation, histone methylation can lead to both, transcriptional activation and inactivation. For example, methylation of histone H3 at lysine 4 (H3K4) characterizes active euchromatin, whereas di- and trimethylation of histone H3 at lysine 27 (H3K27me2/me3) as well as at lysine 9 (H3K9me3) are marks of silent DNA (Egger et al., 2004; Strahl & Allis, 2000). Histone modification offers an enormous spectrum of possible alterations and hence participates in gene regulation.

1.2.3 Epigenetics in cancer

Cancer cells often show altered epigenetic modification patterns and almost every type of human neoplasia shows aberrant DNA methylation such as hypermethylation of promotor

areas that induce a gene switch off. In the majority of all cases, especially genes with antiproliferative effects, so called tumor suppressor genes, are affected. For example, *BRCA1* a DNA repair gene that plays an important role for the development of familiar breast cancer revealed silenced by DNA hypermethylation. (Esteller, 2002, 2007; Jones & Baylin, 2002).

Moreover, the disruption of HAT or HDAC activity as well as the abnormal methylation of histones are involved in cancer development. For example in leukemia or lymphoma different pathways lead to a recruitment of HDACs and hence to inappropriate transcriptional repression (Dhordain et al., 1998; Fenrick & Hiebert, 1998).

Here, also the already mentioned reading proteins take action. Bromodomain containing proteins (BRD) are part of the bromo and extraterminal protein (BET) family. They present an important class of histone modification readers that recognize acetylated lysine residues (Shu & Polyak, 2017). Specific inhibitors of BET proteins such as JQ1 lead to the displacement of BRD from chromatin und thus influence transcription. Using JQ1, Hensel et al. were able to block EWS/FLI1 expression in ES. The treatment inhibited proliferation promoted apoptosis *in vitro* and reduced tumor growth *in vivo* (Hensel et al., 2016). Obviously, those reading proteins play crucial roles in maintaining epigenetic memory and gene transcription.

Recently, the histone methyltransferase enhancer of zeste (Drosophila) homolog 2 (EZH2) revealed to be up regulated in different tumor entities (Kleer et al., 2003; Varambally et al., 2002) as well as in ES. EZH2 is a polycomb group protein (PcG) which together with the embryonic ectoderm development protein (EED) and the scaffold protein suppressor of Zeste (SUZ12) forms the polycomb repressor complex 2 (PRC2). PRC2 preferentially silences genes by methylation of lysine 27 of histone 3 (H3K27). E-cadherin and the cyclin-dependent kinase inhibitor CDKN1C (p57KIP2) are examples of tumor suppressor genes that are direct targets of EZH2 in tumor cells and become silenced through H3K27me3 (Cao et al., 2008; Yang et al., 2009). In ES, the EWS/FLI1 fusion protein mediates oncogenic transformation by EZH2 overexpression. Down-regulation of EZH2 reduces tumorigenicity *in vitro* and *in vivo* (Richter et al., 2009). Obviously, EZH2 plays a key role in ES development. The following investigations try to elucidate the role of distinct microRNAs in ES pathogenesis in particular consideration of EZH2 and EWS/FLI1.

1.3 Micro RNA

MicroRNAs (miRNAs) are endogenous, small, non - protein coding RNA molecules that are involved in posttranscriptional gene regulation processes. In contrast to the initial opinion that all mature miRNAs share the same processing pathways, today multiple discoveries lead to the assumption of miRNA specific differences (Winter, Jung, Keller, Gregory, & Diederichs, 2009).

1.3.1 Biogenesis

The first step of the maturation process is the transcription of the miRNA by RNA polymerase II or III (Bartel, 2004). Therefore, miRNAs are under the control of other different regulators. Besides transcriptions factors such as MYC (O'Donnell, Wentzel, Zeller, Dang, & Mendell, 2005) or TP53 (He et al., 2007) also methylation processes are involved in the regulation of miRNA biogenesis (Lujambio et al., 2008). Additionally, miRNA precursors can be subject to RNA editing. Thereby, the base Adenosine is deaminated and turns into an Inosine so that base pairing properties change. A-to-I-editing of miR-145 for example prevents its further maturation (Yang et al., 2006).

The resulting pri-miRNA, a long primary transcript, also runs through two further maturation steps as shown in figure 1. First, the RNase III type endonuclease Drosha together with the DiGeorge syndrome critical region gene 8 protein (DGCR8) edit the pri-miRNA. This results in a pre-miRNA that is exported into the cytoplasm by the Exportin-5/Ran-GTP complex, followed by the catalysis through the RNA-induced silencing complex (RISC). The miRNA processing and the assembly of the RISC in turn are mediated by the so-called RISC loading complex (RLC). This huge protein complex consists of the RNase Dicer, the double-stranded RNA-binding domain protein (TRBP), PACT (protein activator of protein kinase R) (Li et al., 2006) and an Argonaute protein (Gregory, Chendrimada, Cooch, & Shiekhattar, 2005). TRBP and PACT are not essential for the pre-miRNA processing but they stabilize the RLC and make the procedure easier. Furthermore, they might have an influence on the regulation of the miRNA pathway. Recently, de Vito et al. revealed TARBP2 as a key player in ES cancer stem cell development. Incorrect function of the protein leads to a defect miRNA maturation and therefore favored oncogenic transformation (Vito et al., 2012). At first, the RNase Dicer mediates a cleavage step and generates a 22 nucleotide double-stranded miRNA molecule. Since only one strand presents the guiding strand which

is incorporated into the RISC complex, the other passenger strand is degraded. The difference lies within the thermodynamic stability of the base pair of the 5' ends (Schwarz et al., 2003). The remaining miRNA strand associates with the Argonaute protein 2 (AGO2) whereas the transfer is mediated by a multi protein chaperone complex (Meister, 2013). AGO proteins are highly specialized RNA-binding modules that have endonuclease activity and are essential for miRNA maturation and for miRNA associated gene regulation processes (Diederichs & Haber, 2007). AGO2 recognizes messenger RNA (mRNA) molecules that are complementary to the incorporated miRNA. Depending on the quality of base pairing in the 3' untranslated region (UTR) AGO2 arranges degradation as well as destabilization or inhibition of translation (Filipowicz, Bhattacharyya, & Sonenberg, 2008). In contrast to these results, Vasudevan et al. demonstrated that the interaction of miRNA and AGO2 under special cellular conditions can also lead to an up-regulation of translation (Vasudevan & Steitz, 2007). So far it is little known about miRNA half-life and degradation. RNA-binding proteins that block mRNA access are possible mechanisms to regulate miRNA activity (Kedde et al., 2007).

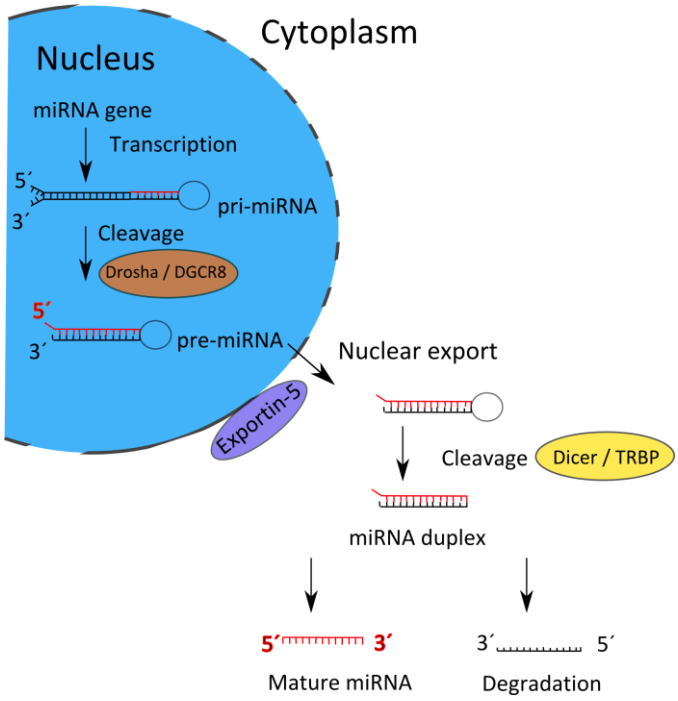

Figure 1: miRNA maturation: Transcription of the miRNA by RNA polymerase II or III. Editing of the pri-miRNA by Drosha and DGCR8 followed by a cleavage step of the pre-miRNA mediated by Dicer. Finally, incorporation into the RISC complex.

1.3.2 miRNAs and cancer

miRNAs have a huge influence on many genes and dysregulation of them has been documented in a variety of human tumors. Causes for abnormal expression can be very different. Chromosomal aberrations such as amplification, deletion or translocation can if they include genomic regions of miRNAs contribute to oncogenic transformation (Zhang et al., 2006). Epigenetic changes can also influence miRNA expression profiles. An altered methylation status can lead for example to a down-regulation of miRNAs that function as a tumor suppressor (Furuta et al., 2010). On the other side miRNAs are able to influence the epigenetic machinery, as well. Fabbri et al. found out that the miR-29 family can regulate the DNA methyltransferase 3A and 3B, frequently up-regulated in lung cancer. The artificial up-regulation of miR-29 normalized the methylation pattern in lung cancer cells and inhibited the tumorigenicity *in vitro* and *in vivo* (Fabbri et al., 2007). Furthermore, miRNAs are capable of altering histone modifications by influencing the expression of HDACs. HDAC1, which is frequently overexpressed in prostate cancer is a direct target of miR-449a. Up-regulation of miR-449a induced cell cycle arrest as well as apoptosis by repressing the expression of HDAC1 (Noonan et al., 2009).

Moreover, it becomes evident that miRNAs are deregulated in almost each type of human cancer whereas expression patterns differ from neoplasia to neoplasia. Not only expression levels show differences but also miRNA biology and downstream targets. In ES miR-221 is characterized to be down-regulated through a repressive function of EWS/FLI1. Downstream targets involve the pro-oncogenic IGF pathway which is thereby deregulated (McKinsey et al., 2011). In contrast, overexpression of miR-221 in prostate carcinoma cell lines revealed to influences the cell cycle inhibitor p27Kip1 and thus showed oncogenic potential (Galardi et al., 2007). However, miRNAs can also be helpful as diagnostic and prognostic tools. Lu et al. showed that miRNA expression patterns can be used to give evidence about the developmental lineage and differentiation state of tumors (Lu et al., 2005). While Robin et al. revealed miR-708 to have an influence on chemoresistence in ES (Robin et al., 2012).

Therefore, miRNAs present an interesting and so far underexplored target for cancer therapy strategies in ES.

1.3.3 Synthetic miRNA mimics and antagomirs

In order to study cancer specific miRNA expression and signaling pathways or to elaborate targeted therapy strategies, non-coding RNA-based oligonucleotides have been developed. These synthetic molecules are either able to mimic mature miRNA (mimic) or to inhibit miRNA function (antimir). As shown in figure 2, Antimirs bind the mature miRNA in competition with cellular target mRNAs leading to functional inhibition of the miRNA and derepression of their direct target (Stenvang, Petri, Lindow, Obad, & Kauppinen, 2012).

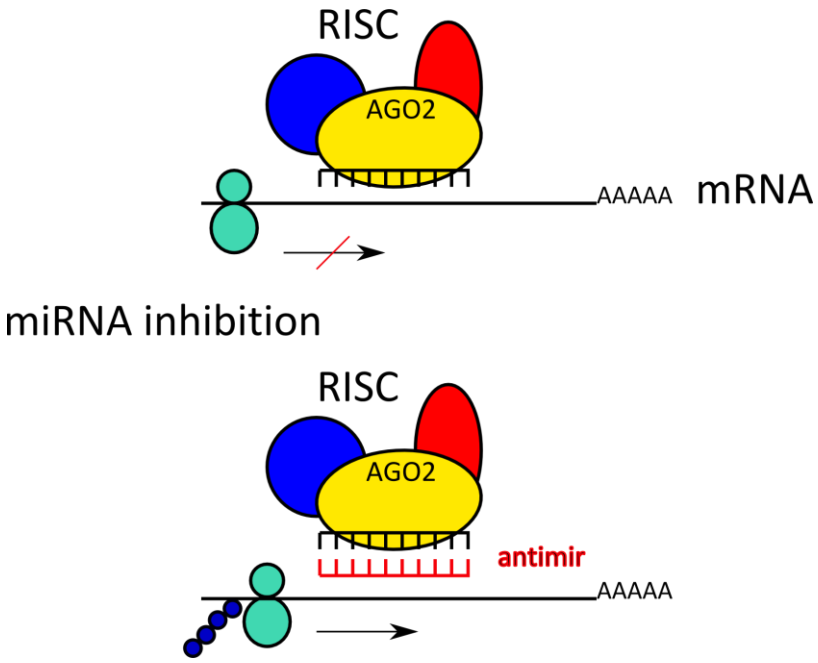

Figure 2: RISC complex with incorporated miRNA: AGO2 mediated inhibition of translation. Chemically modified antimir oligonucleotides sequester the mature miRNA in competition with cellular target mRNAs leading to functional inhibition of the miRNA and derepression of the target (Stenvang et al., 2012).

1.4 Aim of this study and experimental approach

It is the purpose of this doctoral thesis to shed further light on the relevance of miRNAs in ES pathogenesis. Therefore three different miRNAs (miR-203, miR-221, miR-497) previously found as significantly deregulated in an array analysis were selected and their contribution to cell proliferation, metastasis and molecular function were analyzed. Additionally, also epigenetic regulatory mechanisms of these three miRNAs were examined.

In order to get more information about the miRNAs in ES miRNA expression profiles for every miRNA were generated using qRT-PCR. Depending on their individual expression level in ES, cells were transiently treated with a mimic or an inhibitor. The influence of this artificial up- or down-regulation on EZH2 and EWS/FLI1 was evaluated to verify mutually regulation mechanisms. Besides EZH2 and EWS/FLI1 also other epigenetic modifications and their influence on those three miRNAs were examined. Therefore, ES cells were treated with an EZH2 inhibitor, two HDAC inhibitors and an inhibitor of DNA methylation. Changes of miRNA expression levels were assessed using qRT-PCR, while the inhibitor function was validated using Western blot analysis.

Changes caused by those miRNAs were assayed by investigating invasiveness, contact independent growth and proliferation capacity with the help of different *in vitro* assays. Additionally, a xenograft mouse model was utilized to confirm results *in vivo* using ES cell lines, A673 and SK-N-MC, with constitutive overexpression of miR-203.

This work may lead to a better understanding of the role of miRNAs in ES pathogenesis and their regulations. Furthermore, these results will contribute to the long-term aim to explore and validate new ES-specific targets for alternative target-orientated therapeutic strategies.

2. Materials

2.1 List of manufactures

TABLE 1: LIST OF MANUFACTURES

Manufacturers	Location
Abcam	Cambridge, UK
Abbott	Wiesbaden, Germany
Abnova	Taipei, Taiwan
AEG	Nürnberg, Germany
Affymetrix	High Wycombe, UK
Ambion	Austin, TX, USA
Amersham Biosciences	Piscataway, NJ, USA
Applied Biosystems	Darmstadt, Germany
ATCC	Rockyville, MD, USA
B. Braun Biotech Int.	Melsungen, Germany
BD Biosience Europe	Heidelberg, Germany
Becton Dickison (BD)	Heidelberg, Germany
Berthold detection systems	Pforzheim, Germany
Biochrom	Berlin, Germany
Biometra	Göttingen, Germany
BioRad	Richmond, CA, USA
Biozym	Hess. Olendorf, Germany
Brand	Wertheim, Germany
Calbiochem	Darmstadt, Germany
Carestream Health, Inc.	Stuttgard, Germany
Cell Signaling Technology	Frankfurt a. M. , Germany
Charles River Laboratories	Wilmington, MA, USA
Clonetech – Takara Bio Europe	Saint-Germain-en-Laye, France
DSMZ	Braunschweig, Germany
Eppendorf	Hamburg, Germany
Eurofins MWG GmbH	Ebersberg, Germany

Falcon	Oxnard, CA, USA
Feather	Osaka, Japan
Fermentas	St. Leon-Rot, Germany
GE Healthcare	Uppsala, Sweden
Genomed	St. Louis, MO, USA
Genzyme	Neu-Isenburg, Germany
GFL	Segnitz, Germany
Gibco	Darmstadt, Germany
GWL	Würzburg, Germany
Greiner Bio one	Nürtingen, Germany
Hamilton	Bonaduz, Switzerland
Heidolph Instruments	Schwabach, Germany
Invitrogen	Karlsruhe, Germany
Kern	Balingen-Frommern, Germany
Köttermann	Uetze/Hänigsen, Germany
Laborservice	Harthausen, Germany
Leica	Wetzlar, Germany
LMS	Brigachtal, Germany
Lonza	Basel, Switzerland
Macherey-Nagel	Düren, Germany
Mammert	Schwabach, Germany
Merck	Darmstadt, Germany
Metabion	Martinsried, Germany
Millipore	Billerica, MA, USA
Nalgene	Rochester, NY, USA
Nikon	Düsseldorf, Germany
PAA	Cölbe, Germany
Philips	Hamburg, Germany
Qiagen	Chatsworth, CA, USA
R&D Systems	Minneapolis, MN, USA
Roche	Mannheim, Germany

Roth	Karlsruhe, Germany
Santa Cruz Biotechnology	Heidelberg, Germany
Satorius	Göttingen, Germany
Scientific Industries	Bohemia, NY, USA
Scotsman	Milan, Italy
Sempermed	Wien, Austria
Sequiserve	Vaterstetten, Germany
Sigma	St. Louis, MO, USA
Siemens	München, Germany
Systec	Wettenberg, Germany
Taylor-Wharton	Husum, Germany
Techlab	Braunschweig, Germany
Thermo Scientific	Braunschweig, Germany
TKA GmbH	Niederelbert, Germany
TPP	Trasadingen, Switzerland
Whatman	Dassel, Germany
Zeiss	Jena, Germany

2.2 General Materials

TABLE 2: GENERAL MATERIALS

Materials	Manufacturers
Combs (Western blot)	Biometra
Cryovials	Greiner bio-one
Culture dishes (Nuclon™ surface 100mm)	BP Falcon
Cuvettes	Roth
E-plates (96-well)	Roche
Filters for cells, Cell strainer	Falcon
Filter for solution (0,2 µm and 0,45 µm)	Satorius
Flasks for cell culture (25 cm^2, 75 cm^2, 175 cm^2)	Grainer bio-one
Gloves (nitril)	Sempermed
Hypodermic needle (23 G, 30 G)	B. Braun
Pasteur pipettes	Grainer bio-one
Petri dishes	Falcon
Pipettes (2, 5, 10, 25 ml)	Falcon
Pipette tips (10, 100, 200, 1000 µl)	Thermo Scientific
Plates for cell culture (6-well, 24-well, 96-well)	TPP
Plates for invasion-assay (24-well)	BD Bio Science
Plates for qRT-PCR (96-well)	Applied Biosystems
Syringes (27 G x 318``, 0,45 mm x 10 mm)	BD Bioscience
Syringes (GC, 1710LT)	Laborservice
Syringes (Hamilton 100 µl, 250 µl)	Techlab
Syringes (Omnifix-F, 9161406V)	B. Braun
Tubes for cell culture (15, 50 ml)	Falcon
Tubes for molecular biology, safelock (1.5 ml, 2 ml)	Eppendorf
Tubes for FACS™ (5 ml)	Falcon
Whatman paper	Whatman

2.3 Instruments and equipment

TABLE 3: INSTRUMENTS AND EQUIPMENT

Type of device		Manufacturer
Airflow		Köttermann
Autoclave	2540EL	Systec
Autoclave	V95	Systec
Bacteria shaker	Certomat BS-T	Sartorius
Centrifuge	Multifuge 3 S-R	Heraeus
Centrifuge	Biofuge fresco	Heraeus
Controlled-freezing box		Nalgene
Drying cabinet		Memmert
Electrophoresis chamber		Biorad
Flow cytometer	FACSCalibur™	Becton Dickinson
Freezer (-80 °C)	Hera freeze	Heraeus
Freezer (-20 °C)	Cool vario	Siemens
Fridge (+4 °C)	Cool vario	Siemens
Gel documentation	Gene genius	Syngene
Ice machine	AF 100	Scotsman
Incubator	B20	Heraeus
Incubator	Heera cell 150	Heraeus
Liquid Nitrogen Tank	L-240 K series	Taylor-Wharton
Multichannel pipette	10-100 µl	Eppendorf
Heating block	Thermomixer Comfort	Eppendorf
Hemocytometer	Neubauer	Brand
Micropipettes	0.5-10 µl, 10-100 µl, 20-200 µl, 100-1000 µl)	Eppendorf
Microscope (fluorescence)	Axio Vert 100	Zeiss
Microscope	DMIL	Leica
Microwave oven		Siemens, AEG
Mini centrifuge	MCF-2360	LMS
Pipetting assistent	Easypet	Eppendorf

Power supplier	Standard Power Pack P25	Biometra
qRT-PCR cycler	7300 Real-time PCR	Applied Biosystems
Rotator		GLW
Scales	770	Kern
Scales	EW3000-2M	Kern
Semi-dry Transfer Apparatus	Fastblot	Biometra
SDS-PAGE chamber	Minigel-Twin	Biometra
Shaker	Polymax 2040	Heidolph Instruments
Spectrophotometer	GeneQuant II	Amersham Biosciences
Sterile Bench		Heraeus
Water bath		GFL
Western blot documentation	Gel Logic 1500 imaging system	Carestream Health, Inc.
Vortexer	Vortex-Genie 2	Scientific Industries
Water purification system	TKA GenPure	TKA GmbH

2.4 Chemical and biological reagents

TABLE 4: CHEMICAL AND BIOLOGICAL REAGENTS

Reagents	**Manufacturer**
30% Acrylamide	Sigma
Agar	Sigma
Agarose	Invitrogen
Ampicillin	Merck
Ammonium persulfate (APS)	Sigma
β-Mercaptoethanol	Sigma
BCP (1-brom-3-chloropropane)	Sigma
BenchMark™ Prestained Protein Ladder	Invitrogen
Blasticidin	Gibco
Calcein AM	Merck

DEPC (diethyl pyrocarbonate) treated Water	Sigma
1 kb DNA Ladder	Invitrogen
DMEM medium	Invitrogen
DMSO (dimethyl sulfoxide)	Merck
EDTA (ethylenediaminetetraacetate)	Merck
EtBr (Ethidium bromide)	BioRad
Ethanol	Merck
FBS (fetal bovine serum)	Biochrom
37% Formaldehyde	Merck
Gentamycin	Biochrom
Glycerol	Merck
Glycine	Merck
Geneticin	PAA
HBSS (Hank's buffered salt solution)	Invitrogen
HCl (hydrochloric acid)	Merck
HiPerfect Transfection Reagent	Qiagen
Isoflurane	Abbott
Isopropanol	Sigma
KCl (potassium chloride)	Merck
L-glutamine	Invitrogen
Lipofectamine™ 2000 Reagent	Invitrogen
Matrigel matrix	BD Biosciences
Maxima™ Probe / ROX qRT-PCR Master Mix (2 x)	Fermentas
Methanol	Roth
Methylcellulose	R & D Systems
$MgCl_2$ (magnesium chloride)	Invitrogen
NaCl (sodium chloride)	Merck
Na_2HPO_4 (sodium phosphate dibasic)	Merck
NaH_2PO_2 (sodium phosphate monobasic)	Merck

Opti-MEM I Reduced Serum Medium	Invitrogen
PBS 10 x (phosphate buffered saline)	Invitrogen
Peptone	Invitrogen
Polyprene (hexadimethrine bromide)	Sigma
Proteinase K	Sigma
Puromycin	PAA
Ready-Load 1kb DNA Ladder	Invitrogen
RNase A (Ribonuclease A)	Roche
RPMI 1640 medium	Invitrogen
SDS	Sigma
Skim milk powder	Merck
TEMED (N,N,N',N'-Tetramethylethylendiamin)	Sigma
Tris	Merck
Trypan blue	Sigma
Trypsin / EDTA	Invitrogen
Tween 20	Sigma

2.5 Commercial reagent kits

TABLE 5: COMMERCIAL REAGENT KITS

Name	**Manufacturer**
Angiogenesis System: Endothelial Cell Invasion	BD Biosciences
BLOCK-iT™ Lentiviral Pol II miR RNAi Expression system	Invitrogen
ECL-Plus Western Blot Detection System	GE Healthcare
High-Capacity cDNA Reverse Transcription Kit	Applied Biosystems
Human Methycellulose Base Medium	R & D Systems
JETSTAR 2.0 Plasmid Maxiprep Kit	Genomed
NucleoSpin® Plasmid Kit	Macherey-Nagel

MycoAlert Mycoplasma Detection Kit	Lonza
QIAEX II Gel Extraction Kit	Qiagen
TRI Reagent RNA Isolation Kit	Ambion
TaqMan® Gene Expression Assays	Applied Biosystems
TaqMan® MicroRNA Assays	Applied Biosystems
TaqMan® MicroRNA Reverse Transcription Kit	Applied Biosystems

2.6 Media, buffers und solutions

TABLE 6: CELL CULTURE MEDIUM UND UNIVERSAL SOLUTIONS

Name	**Ingredients**
Standard tumor medium	500 ml RPMI 1640 10% FBS, 100 µg/ml gentamycin
4% formaldehyde	4% Formalin, 55 mM Na_2HPO_4 , 12 mM NaH_2PO_4 , 2 H_2O
FACS staining buffer	2% FBS, 0.05% NaN_3 dissolved in 1 x PBS

TABLE 7: BUFFER AND GEL FOR DNA/RNA ELECTROPHORESIS

Name	**Ingredients**
TAE running buffer	50 x TAE: 2 M Tris, 10% EDTA (0.5 M), 5.71% HCL
Electrophoresis gel	200 ml TAE (1 x), 1% agarose, 3 µl EtBr

TABLE 8: BUFFERS AND SOLUTIONS FOR CELL CYCLE ANALYSIS

Name	**Ingredients**
Sample buffer	0.1% Glucose (w/v) in 1 x PBS, 0.22 µm filtration, stored at 4 °C
PI staining solution	50 µg/ml Propidium iodide and 100 U/ml RNase A in sample buffer

TABLE 9: BUFFERS AND GELS FOR WESTERN BLOT ANALYSIS

Name	Ingredients
Laemmli buffer (3 x)	0.5 M Tris/HCL pH 6.8, 10% SDS, 45% Glycerol, 0.1% Bromphenol blue
SDS running buffer (1 x)	25 mM Tris, 200 mM Glycine, 0.1% (w/v) SDS
Separating buffer (4 x)	1.5 M Tris, 0.4% SDS, adjusted to pH 8.8 with HCl
Separating gel (8-12.5 %)	10%: 3.33 ml 30% Acrylamide / Bis, 2.5 ml Separating Buffer (4 x), 4.17 ml water, 50 µl APS (10%), 20 µl TEMED
Stacking buffer (4 x)	0.5 % Tris, 0.4% SDS, adjusted to pH 6.8 with HCl
Stacking gel (4.5 %)	750 µl 30% Acrylamide / Bis, 1.25 ml Stacking Buffer (4 x), 3 ml water, 50 µl APS (10%), 20 µl TEMED
Transfer buffer (5 x)	25 mM Tris pH 8.3, 192 mM Glycine
TBS (10 x)	0.5 M Tris-HCL pH 7.4, 1.5 M NaCl
TBS-T	1 x TCBS including 0.05% (v/v) Tween 20

2.7 Antibodies

TABLE 10: ANTIBODIES FOR WESTERN BLOT

Antibody	Source	Dilution	Product No.	Manufacturer
Anti-EZH2	rabbit	1:1000	5246S	Cell Signaling
Anti-H3K27me3	rabbit	1:5000	C15410199	Diagenode
Anti-H3 K9/K14 ac	rabbit	1:3000	06-599	Milipore
Anti-H3	rabbit	1:5000	Ab1791	Abcam
Anti-rabbit IgG HRP	bovin	1:5000	sc-2370	Santa-Cruz

2.8 Small interfering RNAs

TABLE 11: SMALL INTERFERING RNA USED FOR TRANSIENT TRANSFECTION

siRNA Name	Target Sequence (5'-3')
Control siRNA	AAT TCT CCG AAC GTG TCA CGT
EZH2_2 siRNA	AAG CAA ATT CTC GGT GTC AAA
EZH2_7 validated siRNA	AAC CAT GTT TAC AAC TAT CAA

2.9 miScript miRNA mimic / inhibitor

Mimics and inhibitors were obtained from Qiagen.

TABLE 12: MISCRIPT MIRNA MIMIC / INHIBITOR USED FOR TRANSIENT TRANSFECTION

Mimic / inhibitor Name	Target Sequence (5'-3')
Syn-hsa-miR-203a-3p miScript miRNA Mimic	GUG AAA UGU UUA GGA CCA CUA G
Syn-hsa-miR-221-5p miScript miRNA Mimic	ACC UGG CAU ACA AUG UAG AUU U
Anti-hsa-miR-221-5p miScript miRNA Inhibitor	ACC UGG CAU ACA AUG UAG AUU U
Anti-hsa-miR-497-5p miScript miRNA Inhibitor	CAG CAG CAC ACU GUG GUU UGU

2.10 Oligonucleotides for lentiviral gene transfer

Oligonucleotides used for lentiviral gene transfer were ordered from Metabion International AG.

TABLE 13: OLIGONUCLEOTIDES USED FOR LENTIVIRAL GENE TRANSFER

Name	Sequence (5'-3)
hsa-miR-203a-3p	GTG AAA TGT TTA GGA CCA CTA G

2.11 Primers for qRT-PCR

TABLE 14: PRIMERS FOR QRT-PCR

Name	Sequence (5'-3')
EWS/FLI1 for	TAG TTA CCC ACC CAA ACT GGA T
EWS/FLI1 rev	GGG CCG TTG CTC TGT ATT CTT AC

2.12 Gene expression assays for qRT-PCR

2.12.1 TaqMan Gene Expression Assays

All TaqMan Gene Expression Assays were obtained from Applied Biosystems.

TABLE 15: TAQMAN GENE EXPRESSION ASSAYS

Gene	Assay ID
EZH2	Hs00544830_m1
GAPDH	Hs99999905_m1

2.12.2 TaqMan MicroRNA Assays

All TaqMan MicroRNA Assays were obtained from Applied Biosystems.

TABLE 16: TAQMAN MICRORNA ASSAYS

microRNA	Assay-name
hsa-miR-203	hsa-miR-203a-3p
hsa-miR-221	hsa-miR-221-5p
hsa-miR-497	hsa-miR-497-5p

2.13 Expression vector

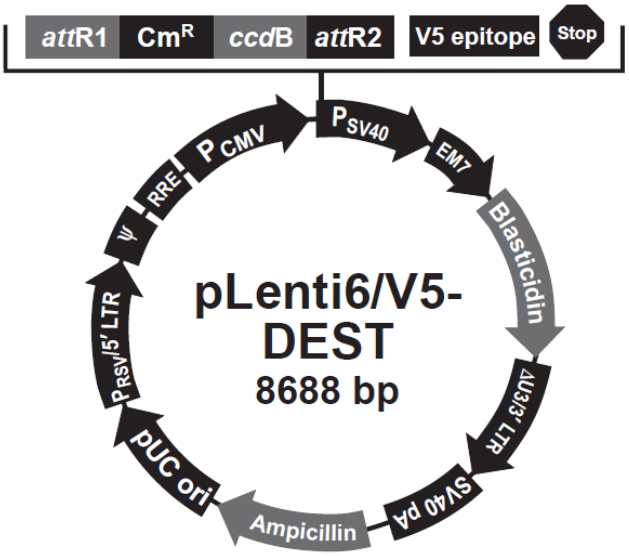

Figure 3: Lentiviral destination vector for miRNA expression produced by invitrogen

2.14 Human cell lines, bacterial strain and mouse strains

2.14.1 Human cell lines

All Human cell lines were provided by the German Collection of Microorganisms and Cell Cultures (DSMZ), except for A673, which was purchased from ATCC (LGC Standards). Human primary cell line SB-KMS-KS1 was generated in the laboratory. Packaging cell line 293FT for letivirus production was obtained from Invitrogen.

TABLE 17: DESCRIPTION OF UTILIZED HUMAN CELL LINES

Cell line	Description
A673	ES cell line (type 1 translocation), established from the primary tumor of a 15-year-old girl (Giard et al., 1973), p53 mutation
cALL2	Human B cell precursor leukemia, established from the peripheral blood of a 15-year-old Caucasian girl with acute lymphoblastic leukemia (cALL)
L87	Immortalized with SV40 large T-antigen (Moosmann, Hutter, Moser, Krombach, & Huss, 2005)2005)
MG-63	Osteosarcoma cell line, established from the bone of a 14-year-old Caucasian boy.
MHH-ES1	ES cell line (type 2 translocation), established from the ascites of a 12-year-old Turkish boy with a tumor of the left pelvis and additional peritoneal metastases
MHH-NB11	Neuroblastoma cell line, established from an adrenal metastasis of a 4-year-old Caucasian boy
Nalm6	Human B cell precursor leukemia, established from the peripheral blood of a 19-year-old man with acute lymphoblastic leukemia (ALL) in relapse
RD-ES	ES cell line (type 2 translocation), established from the primary tumor of a 19-year-old Caucasian man localizised in the humerus
REH-1	Established from the peripheral blood of a 15-year-old girl with acute lymphoblastic leukemia

SB-KMS-KS1	ES cell line (type 1 translocation), established from an extraosseous inguinal metastasis of a 17-year old girl (new nomenclature, originally designated as SBSR-AKS)
SH-SY5Y	Neuroblastoma cell line, established from a bone marrow biopsy of a 4-year-old girl with metastatic neuroblastoma
SK-ES1	ES cell line (type 2 translocation), established from the Ewing Tumor of an 18-year-old man
SK-N-MC	ES cell line (type 1 translocation), established from the supraorbital metastases of a 14-year-old girl (Askin's tumor, related to ES)
TC-71	ES cell line (type 1 translocation), established in 1981 from a biopsy of recurrent tumor of a 22-year-old man with metastatic ES (humerus)
U2OS	Osteosarcoma cell line, established from the bone of a 15-year-old Caucasian girl
VH54.2	Immortalized with SV40 large T-antigen (Moosmann et al., 2005)
697	Human B cell precursor leukemia, established from bone marrow of a 12-year-old boy with ALL in relapse

2.14.2 Bacterial strains

The following bacterial strains were used for plasmid enrichment to generate cells with stable mimic through lentiviral gene transfer.

TABLE 18: DESCRIPTION OF UTILIZED BACTERIA STRAINS

***E. coli* strain**	**Genotype description**	**Origin**
One Shot® TOP10 Chemically Competent	F- *mcrA* Δ(*mrr-hsd*RMS-*mcr*BC) φ80*lac*ZΔM15 Δ *lac*X74 *rec*A1 *ara*D139 Δ(*araleu*)7697 *gal*U *gal*K *rps*L (StrR) *end*A1 *nup*G	Invitrogen
One Shot® Stbl 3 Chemically Competent	F^-*mcr*B *mrrhsd*S20(r_B^-, m_B^-) *rec*A13 *sup*E44 *ara*-14 *gal*K2 *lac*Y1 *pro*A2 *rps*L20(Str^R) *xyl*-5 λ^-*leumtl*-1	Invitrogen

2.14.3 Mouse strains

TABLE 19: DESCRIPTION OF UTILIZED MOUSE STRAINS

Mouse strain	Characteristics	Origin
BALB/c RAG2$^{-/-}$YC$^{-/-}$	No T-lymphocyte and B-lymphocyte generation and no NK cell function	Central Institute for Experimental Animals (Kawasaki, Japan)

The Recombination activating gene 2 (Rag2)-*gamma(c)* knock-out (Rag2$^{-/-}$γc$^{-/-}$) mouse is an immunodeficient model that can be used in studies to test *in vivo* conditions. This gene manipulated mouse strain was generated by backcrossing of two immunocompromised mouse models, the gamma(c) knock-out and the Rag2 knock-out mice. The homozygous *gamma(c)* knock-out mice has no *gamma(c)* receptor gene, why the development of lymphocytes is severely compromised. As a consequence, natural killer (NK) cell population is severely decreased in these mice, but they do have a small number of T- and B-lymphocytes. In order to completely eliminate the T and B cell population, the *gamma(c)* knock-out mouse was back-crossed onto the *Rag2* knock-out mouse. Homozygous Rag2 knock-out mice do not have several exons of the *Rag2* gene, resulting in the inability to initiate V(D)J rearrangement which is responsible for the viability of antibodies. Therefore, these *Rag2* knock-out mice are incapable of generating any T- and B-lymphocytes (Goldman et al., 1998).

As a result, the back-crossed Rag2$^{-/-}$γc$^{-/-}$ mice had neither T-lymphocytes and B-lymphocytes nor NK cell functions.

3. Methods

3.1 Cell culture

ES cell lines A673, SK-N-MC, TC-71, SB-KMS-KS, SKES1, RDES and MHHES were cultured in RPMI medium with 10% fetal bovine serum (FBS) and 1% Gentamycin at 37 °C (5% CO_2) in a humidified atmosphere. In middle-sized culture flasks with 75 cm^2 adherent surface the volume of medium was 20ml and in large-sized culture flasks with 175 cm^2 adherent surface it was 25ml. Approximately every three days since cells have grown confluent the medium had to be replaced and the cells were split from 1:2 to 1:10. Therefore, cells were treated with 3 ml und 4 ml Trypsin for 5 min. at 37 °C (5% CO_2) in order to remove the adherent cells from the culture flasks. Then detached cells were resolved in 10ml RPMI medium and centrifuged at 1500 rpm for 5 min. to spread them finally in new culture flasks. Other adherent cell lines such as U2OS, MG-63 as well as SH-SY5Y and MHH-NB11 were cultured in the same manner. The cALL tumor cell lines 697, cALL, Nalm6 and REH-1 which grow in suspension were cultured in 20 ml RPMI medium with 10% fetal bovine serum (FCS) and 1% Gentamycin at 37 °C (5% CO_2) in a humidified atmosphere.

The lentivirus packaging cell line 293FT was cultured in a large-sized culture flask with 25 ml of D-MEM medium containing 10% FBS, 2mM L-glutamine, 0.1 mM MEM Non-Essential Amino Acids, 1mM MEM Sodium Pyruvate and 1% Gentamycinin. Cells grew as well at 37 °C (5% CO_2) in a humidified atmosphere.

To prepare cryovials for long-time storage in liquid nitrogen (-192°C) cells were counted and re-suspended in FBS with 10% DMSO. At first the cryovials were put in controlled freezing boxes for 12-18h at -80 °C. Next to that they were moved into the liquid nitrogen freezer for long-time storage. For re-culturing the cryopreserved cells vials were thawed at room temperature and the contend was replaced in a 50 ml Falcon tube for centrifugation at 1500 rpm for 5 min. After re-suspension of the cell pellet, cells were spread in fresh pre-warmed culture medium in small-sized culture flasks.

A Neubauer hemocytometer was used to count cell numbers and cell viability was assessed by trypan blue (Sigma) exclusion method. Cultured cells were checked routinely for mycoplasma contamination using MycoAlertTM Mycoplasma Detection Kit (Lonza) according to manufacturer's instructions.

3.2 RNA Isolation using TRI Reagent RNA Isolation Kit

To isolate RNA from frozen tissues or cultured cells TRI Reagent RNA Isolation Kit was used in accordance to manufacturer's instructions (Ambion Manual Version 0610).

Therefore, the tissue sample was homogenized in 1 ml TRI Reagent solution per 5-10 x 10^6 cells and incubated for 5 min. at room temperature. Afterwards 100 µl of BCP (1-bromo-3-chloropropane) per 1 ml TRI Reagent was added and samples were mixed very well by vortexing. After a second incubation of 10 min. the samples were centrifuged at 12.000 x g for 13 min. and 4 °C so that the adjacent aqueous layer could be removed and subsequently precipitated through the addition of 500 µl isopropanol per 1 ml TRI Reagent and a second round of centrifugation at 12.000 x g for 8 min. The precipitated RNA pellet was washed with 1 ml 75% ethanol per 1 ml of TRI Reagent and centrifuged again at 12.000 x g for 5min. After the ethanol was poured of the remaining pellet was let air-dried for 5 – 10 min. and dissolved in 40 µl RNase-free water. Finally, the RNA concentration was measured at 260 nm and RNA was stored at -80°C for later on analysis.

3.3 cDNA Synthesis

In order to analyze gene expression by quantitative real time PCR, RNA had to be reverse transcribed into a complementary single-stranded DNA (cDNA) transcript. Therefore, the High-Capacity cDNA Reverse Transcription Kit was mixed with 14.2 µl RNA solution containing 1 µg RNA solution and 2 µl of 10 x RT Random Primers, 2 µl of 10 x RT Buffer, 1 µl of 25 x dNTP mix (100mM) and 0,8 µl of MultiScribe ™Reverse Transcriptase (50 U/µl). The cDNA was synthesized under the following conditions: 10 min. 25 °C; 120 min. 37 °C; 5 min. 85 °C; ∞ 4 °C. Synthesized cDNA was either instantly used for examination of gene expression or stored at -20 °C.

3.4 Quantitative Real-Time PCR (qRT-PCR)

The newly synthesized cDNA was quantified to obtain information about gene expression as the amount of cDNA correlated to the amount of cellular mRNA using qRT-PCR. The reaction was performed by using Maxima™ Probe/ROX qPCR Master Mix (2x) that contains Hot Start Taq DNA Polymerase, PCR buffer and dNTPs. Additionally, specific TaqMan Gene Expression Assays (Applied Biosystems) were utilized, which consists of two unlabeled PCR primers and a FAM™ dye labeled TaqMan® MGB probe. For each sample 10 µl of the master

mix, 1 µl of the desired primer and 0.5 µl of cDNA template were mixed in 96 - well plates und adjusted to a final volume of 20 µl with RNase-free water. Gene expression profiles were normalized to the mRNA levels of the housekeeping gene *glyceraldehyde 3-phosphate dehydrogenase* (*GAPDH*) and calculated using the 2^{-ddCt} method.

3.4.1 Detection of EWS/FLI1

Gene Expression Assays for the detection of *EWS/FLI1* levels were designed and used as followed: 10 µl Maxima™ Probe/ROX qPCR Master Mix (2 x), 9 µl of nuclease-free water were mixed in 96-well plates with 0.6 µl of each primer (0.3 µM) and 0.4 µl of FAM probe (0.2 µM). Afterwards 0.5 µl of the cDNA template was added. Gene expression profiles were normalized to the mRNA levels of the housekeeping gene *glyceraldehyde 3-phosphate dehydrogenase* (*GAPDH*) and calculated using the 2^{-ddCt} method.

TABLE 20: GENE EXPRESSION ASSAY TO DETECT EWS-FLI1 MRNA BY QRT-PCR

Sense primer	5'-TAG TTA CCC ACC CAA ACT GGA T-3'
Antisene primer	5'-GGG CCG TTG CTC TGT ATT CTT AC-3'
FAM probe	5'-FAM-CAG CTA CGG GCA GCA GAA CCC TTC TT-TAMRA -3'

3.5 MicroRNA analysis

MicroRNA (miRNA) quantification was performed using the TaqMan MicroRNA Reverse Transcription Kit and specific TaqMan™ MicroRNA Assays. Similar to the synthesis of cDNA from mRNA the first step involved the generation of a master mix (MM) containing 1.5 µl of 10 x RT Buffer, 0.15 µl of dNTP mix, 0.19 µl of RNAse Inhibitor (20U/µl), 4.16 µl of nuclease-free water and 1 µl of MultiScribe ™Reverse Transcriptase (50 U/µl). Then 10 ng total RNA solution was added to 3 µl miRNA specific RT primers, 4 µl water and 7 µl MM. The cDNA was synthesized under the following conditions: 30 min. 16°C; 30 min. 42°C; 5 min- 85°C; ∞ 4°C. For qRT-PCR analysis 1.33 µl of cDNA was added to 10 µl Maxima™ Probe/ROX qPCR Master Mix (2 x), 7.67 µl of nuclease-free water and 1 µl of specific FAM-labeled TaqMan™ MicroRNA Expression Assay to a final volume of 20 µl. Gene expression profiles were normalized to the small nucleolar RNA (snoRNA) RNU48 and calculated using the 2^{-ddCt} method. Mean values and standard deviations of duplicates were analysed using Microsoft *Excel*.

3.6 Transient RNA interference

For transient RNA knock down and transient mimic of miRNAs in 100 mm dishes, 3 x 10^6 cells were seeded into a final volume of 12 ml including 3.6 µl siRNA (5nM) or 3 µl mimic (5nM) and 36 µl or 30 µl HiPerfect transfection reagent respectively for 72 hours. Furthermore, to inhibit miRNAs transiently, 30 µl inhibitor (50nM) and 60 µl HiPerfect transfection reagent were mixed. To verify the change in gene expression, RNA was isolated and analyzed by qRT-PCR. All experiments were carried out along with a negative control for siRNAs (Qiagen) that has no homology to any known mammalian gene as well as a control for miRNA changes which contained only medium and HiPerfect Transfection reagent.

3.7 Lentivirus mediated stable RNA interference

The BLOCK-iT ™ Lentiviral POL II miR RNAi Expression System (Invitrogen) was used to generate ES cell lines bearing a constitutive higher expression of miRNAs. Therefore synthetic oligonucleotides which corresponded to the mature 3p miRNA sequence were cloned into a pLenti6/V5-DEST lentiviral vector. In brief, synthetic oligonucleotides were annealed to generate double strand (ds) oligonucleotides and then ligated into the pcDNA™6.2-GW/EmGFP-miR expression vector. The out there originating construct was transformed into chemically competent TOP10 *E. coli* bacteria, multiplied and finally purified using NucleoSpin® Plasmid Kit according to manufacturer's instructions (Macherey-Nagel Manual 03/2005/ Rev 02). After testing the correct integration of ds oligonucleotides into the vector by sequencing the expression vector was linearized by digestion through the EAgI restriction enzyme and ligated into the pLenti6/V5-DEST lentiviral vector. The resulting product was again transformed into chemically competent Stbl3™ *E.coli* and plasmid DNA was purified using NucleoSpin® Plasmid Kit. Next, the construct was transduced into 293FT packaging cells and viral supernatant was isolated 48h after transfection. Viral supernatant was immediately used to perform transduction into ES cell lines. Therefore, 1 x 10^5 cells of the cell line A673 and 1 x 10^6 cells of SK-N-MC were spread into six well culture plates and incubated for 24h at 37 °C (5% CO_2) in a humidified atmosphere. Subsequently 1ml of the viral supernatant and 6 µg/ml polybrene were added and incubated for 24 - 48 h under normal culture conditions.

The viral supernatent was removed after 48h. Selection of infectants was made using 10 µg Blasticidin per 1ml RPMI medium and by qRT-PCR in comparison to the negative control.

3.8 xCELLigence proliferation assay

To measure viable cell proliferation in real-time cells were plated on an impedance-based 96 well plate (xCELLigence, Roche/ACEA Biosciences) which uses changes in electrical impedance based on the interaction of adherent cells with electrode plates as the readout to measure cell growth (Ke, Wang, Xu, & Abassi, 2011). The measured changes are displayed as arbitrary cell index values.

For A673 7.3 x 10^3 cells and 1 x 10^4 cells for SK-N-MC were seeded into the E-plate together with 200 µl medium and cultured for maximal 168h whereby the system measured the impedance periodically every hour.

To dissect the influence on proliferation after the transient tranfection, with mimic or inhibitor, the medium was substituted with HiPerfect and the corresponding siRNA or mimic to ensure a steady influence on miRNA expression.

3.9 Invasion assay

To get more information about the ability of ES cells to grow invasively the BioCoat™ Angiogenesis System: Endothelial Cell invasion (BD Biosciences) was used. According to the manufacturer`s instructions the plate was allowed to adjust to room temperature prior to use. Then the plate was treated with 500 µl of pre-warmed RPMI medium without FBS to rehydrate for 45 min at 37 °C (5% CO_2). Subsequently the RPMI medium was removed and replaced by new medium containing 5 x 10^4 cells. Finally the single wells were filled up with 750 µl medium whereby 10% FBS served as chemoattractant. After the incubation time of 48h at 37 °C (5% CO_2) in a humidified atmosphere the medium was removed and the invasive cells were stained with 4 µg/ml Calcein AM solution in pre-warmed HBSS (Hank's buffered salt solution) with 0.15% DMSO and incubated for 90 min at 37 °C (5% CO_2) in a new 24-well plate. Cells were imaged by fluorescence microscopy using a Zeiss AxioVert 100 with attached AxioCam MRm and the visualizing program AxioVision Rel. 4.7 (Carl Zeiss). Photographed invasive cells were then counted using the image processing software *Fiji* and evaluated by Microsoft *Excel*.

3.10 Colony forming assay

To demonstrate the ability of tumor cells to grow contact - independently 1 x 10^4 cells were re-suspended in in 300 µl cell resuspension solution and seeded in duplicate into a 35 mm plate containing 1.5 ml methylcellulose-based media (R&D Systems). Thereafter the assay was cultured for 10 – 14 days at 37 °C (5% CO_2) in a humidified atmosphere. The grown cell colonies were photographed and then counted using Fiji.

3.11 Cell cycle analysis

To obtain detailed information about cell cycle condition of cells a cell cycle analysis was performed using flow cytometry and propidium iodide (PI) staining. As this works as a DNA intercalating agent it emits a fluorescence signal after excitation by a 488 nm laser that correlates with the amount of DNA it contains. This observed signal allows differentiation between phases of cell cycle, as the fluorescence of cells in the G_2/M phase is twice as high as that of cells in the G_0/G_1 phase because of DNA duplication during intermediate S phase. The first step of analysis comprised a two times washing process with cold sample buffer and the fixation of cells in 1 ml ice-cold 70% ethanol that was added drop by drop while vortexing. Afterwards all samples had to spend at least 18h at 4 °C for maximum resolution. During the second step the cells were centrifuged and re-suspended in 1 ml staining buffer containing RNase A and PI to remove any remaining RNA. Then, after an incubation time of 30-60 min. at room temperature with continuous gentle rocking the cells could be analyzed using a FACSCalibur™flow cytometer.

3.12 Inhibitors of epigenetic mechanisms

3.12.1 EZH2 inhibitor treatment

The inhibitor GSK126 inhibits the catalytic site of EZH2. For this purpose 2 x 10^6 cells were seeded in 100 mm dishes with 10ml RPMI standard tumor medium. Then 2 µM GSK126 were added and the dishes incubated for 72h at 37 °C (5% CO_2) in a humidified atmosphere. GSK669A served as negative control.

3.12.2 HDAC inhibitor treatment

For the inhibition of histone deacetylase (HDAC) two different inhibitor were taken. Trichostatin A (TSA) is a pan-HDAC inhibitor and MS-275 preferentially inhibits HDAC1 over HDAC3. Therefore 4 x 10^6 cells were seeded into 100 mm dishes with 10 ml RPMI standard tumor medium and treated for 24h at 37 °C (5% CO_2) in a humidified atmosphere with 100 nM TSA and MS-275, respectively.

3.12.3 Inhibition of DNA-methylation

To prevent DNA-methylation 2 x 10^6 cells were seeded into 100 mm dishes with 10 ml RPMI standard tumor medium and treated with 2 µM of the DNA methyltransferase (DNMT) inhibitor 5-Aza-Cytidine (5-AzaC) for 72h at 37 °C (5% CO_2) in a humidified atmosphere.
To evaluate gene expression after each treatment RNA was isolated, cDNA transcribed and finally analyzed by qRT-PCR. Additionally, proteins were isolated to check protein expression levels by Western blot analyses.

3.13 Western blot analysis

To analyze protein levels cells were trypsinized, counted and 1-2 x 10^6 cells were resuspended in 200/400 µl 2X Laemmli-buffer (containing 50µl ß-mercaptoethanol per 1ml 2X Laemmli). Subsequently, samples were incubated at 70°C for 10min. to denature proteins. Lysates were then homogenized using a 23 gauge needle and centrifuged for 5 min at 14000 rpm. Samples were stored at -80 °C or immediately processed for SDS-polyacrylamide gel electrophoresis (SDS-PAGE).
20 µl of denatured protein lysates were therefore transferred to the SDS-PAGE and electrophoresis was carried out at 120V for 1-2h. Molecular weight of the separated proteins was determined by comparing with a prestained molecular weight standard.
For precise detection of specific proteins by compatible antibodies, proteins had to be transferred onto a membrane. Hence, the gel and a methanol-activated Hybond-P PVDF membrane were placed between Whatman filter papers (soaked in 1 x transfer buffer) and transfer was done under semi-dry conditions at 0.8 mA/cm_2 for 1.5h in a blotting device. After that unspecific binding sites were blocked by shaking the membrane in 5% skim milk substituted with 0.05% Tween20 for 1h at room temperature. Afterwards the membrane was treated with the first antibody targeting the protein of interest. Antibodies were

diluted according to the manufacturer's instructions in 5% skim milk substituted with 0.05% Tween20 and incubated at 4 °C over night. The next day the membrane was washed thrice (10 min. per wash) in 1X TBS-T and once in 5% skim milk substituted with 0.05% Tween20 before it was incubated for 1h with horseradish peroxidase (HRP) coupled secondary antibody in 5% skim milk substituted with 0.05% Tween20. After two further washing steps in 1X TBS-T and only one in 1X TBS the antibody-antigen complex was detected using the ECL-Plus Western Blotting Detection System (GE Healthcare Booklet RPN2132PL Rev D 2006). This system is based on the oxidation of a Luminogen by HRP and peroxide with the result of a chemoluminescent signal detectable by a CCD camera. Signals of antibody-antigen complexes were detected with the Gel Logic 1500 imaging system and analyzed with Kodak Molecular Imaging Software (Version 5.0).

3.14 *In Vivo* experiments

To examine local tumor growth *in vivo,* 2 x 10^6 cells were taken up in 0.2ml 1X PBS and as soon as possible injected subcutaneously into the inguinal region of immune deficient Rag2$^{-/-}\gamma c^{-/-}$ using a 26-gauge needle attached to a 1 ml syringe. Tumor size was determined every day until it reached a size > 1 cm^3 (determined with a caliper). Those mice were considered as positive and sacrificed. Tumors were excised and RNA was prepared for gene expression analysis *ex vivo.*

To give evidence about metastatic spread, ET cells were injected in a volume of 0.2 ml into the tail vein of immunodeficient Rag2$^{-/-}\gamma c^{-/-}$ mice using a 30-gauge needle. Mice were euthanized after four to five weeks and metastatic spread was examined in individual organs. Therefore, all macroscopically apparent metastases within an organ were counted.

3.15 Statistical analysis

The presented data are mean ± SD as indicated. Differences were analyzed by unpaired two-tailed t-test as indicated using *Excel* (Microsoft), or *Prism 5* (GraphPad Software); p values < 0.05 were considered statistically significant.

4. Results

4.1 Non-coding RNAs in ES, previous results

In a previous analysis Burdach et al. described epigenetic mechanisms to be involved in Ewing sarcoma (ES) pathogenesis. They observed that especially the methyltransferases EZH2 is regulated by EWS/FLI1 and plays a key role in the maintenance of stemness and malignancy in ES (Burdach et al., 2009). Next to EZH2, Plehm et. al. found microRNAs (miRNAs) to be regulated by epigenetic mechanisms: Especially miR-221 was shown to be significantly deregulated by the epigenetic machinery and thus needed further analysis to study possible gene regulation interactions (Plehm, 2011).

But not only miRNAs were examined. Additionally, Argonaute proteins (AGO) were studied and found to play an important role for miRNA maturation and function.

In her studies, Plehm et al. first observed miR-221 to be up-regulated in ES cell lines as compared to other pediatric tumor cell lines. In a next step, they looked at AGO2 and found that its knock down inhibited local tumor as well as invasive growth and more importantly led to the reduction of miR-221 expression levels. Further, they were able to demonstrate that EZH2 influenced AGO2 expression. Concluding that overexpressed EZH2 influences AGO2 and thus up-regulates miR-221 which subsequently promotes a highly malignant phenotype of ES (Plehm, 2011). Here we tried to further advance this hypothesis by further investigating miR-221.

Furthermore, Plehm et al. examined direct interaction of EZH2 and microRNAs. Therefore, they used ChIP-on-chip promoter array analysis to detect promoter regions of those miRNAs that are influenced by EZH2. More precisely, the expressional fold change of several miRNAs after either high EZH2 expression or EZH2 knock down was examined. As an indicator for the EZH2 level the change in H3K27me3 was used.

Thereby, miR-497 revealed the most abundant change: a significantly reduced H3K27me3 level at its promoter region upon EZH2 suppression (see table 21).

TABLE 21: MICROARRAY DATA: CHANGES OF SEVERAL MIRNAS AFTER EZH2 KNOCK DOWN

miRNA	**Fold differences EZH2 high/low**
	H3K27me3 mark
miRNA-124a-2	2.05
miRNA-185	1.60
miRNA-199a-1	1.59
miRNA-423	1.52
miRNA-497	**2.40**
miRNA-516-4	1.57

Additionally, they examined EZH2 binding to the promotor region of miR-203 and found that upon EZH2 repression there was less binding to the promotor region but no reduction of H3K27me3 (Plehm, 2011). This indicates that there is an alternative way of regulation by EZH2 apart from simple histone modification.

Taking these previous results into account, this thesis tried to further evaluate the role of miR-203, miR-497 and miR-221 in ES.

4.2 RNU48 as a housekeeping gene for normalization of miRNA qRT-PCR expression data

miRNA expression levels are cell type specific and subject to environmental conditions of the cell of use. Therefore, it is necessary to normalize data and adjust variabilities in miRNA and cDNA quantity or other uncertainties (Peltier & Latham, 2008). For this purpose, constantly expressed reference genes need to be validated. Small-nucleolar RNAs (snoRNAs) are non-protein coding RNAs with different molecular functions, like guiding the site-specific modification of nucleotides in target RNAs (Mattick & Makunin, 2005) and are therefore supposed to be constantly expressed.

To identify genes that do not change expression in all of our experiments we evaluated three previously noted (Gee et al., 2011) possible housekeeping genes (RNU48, RNU19 and RNU6B). The expression of the three potential candidate genes were determined by qRT-PCR after the treatment with miRNA mimics or inhibitors. By doing so, RNU48 showed a stable expression with only minor changes in both cell lines and will therefore serve as a housekeeping gene in all following experiments (see figure 4).

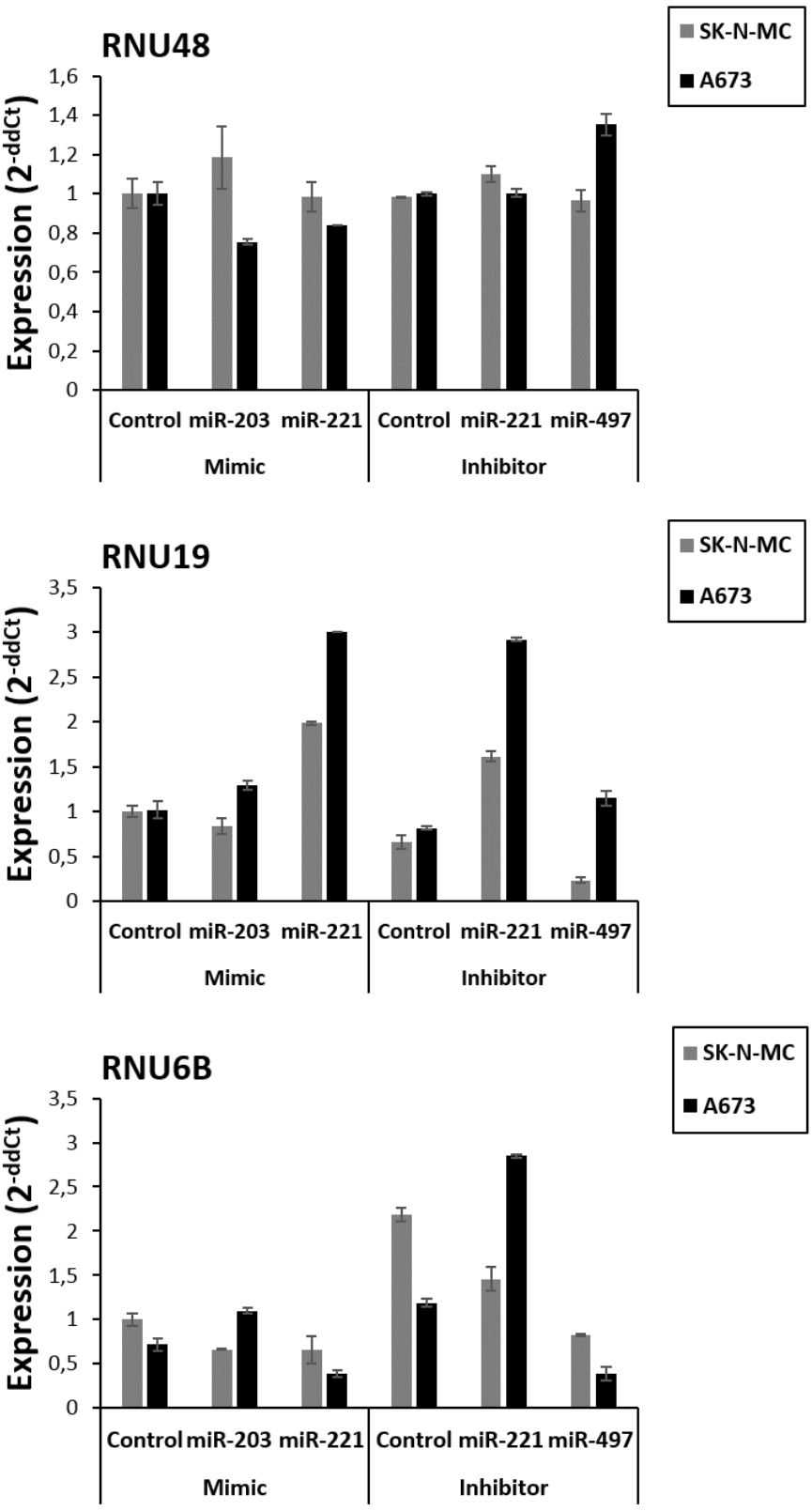

Figure 4: qRT-PCR analysis of three different housekeeping genes. Expression of RNU48, RNU19 and RNU6B was analyzed in 2 different cell lines A673 and SK-N-MC by qRT-PCR. Both cell lines were treated for 24 hours with either mimic or inhibitor, and expressional changes were analyzed. While RNU6B and RNU19 showed volatile expression patterns for mimic and inhibitor, RNU48 showed the most stable expression pattern and was therefore selected as housekeeping gene for all further experiments.

4.3 The role of miR-203 in Ewing sarcoma pathogenesis

4.3.1 Expression of miR-203 in primary ES cell lines is down-regulated

To study ES specific expression levels of miR-203 by qRT-PCR several ES cell lines were analyzed and compared to other pediatric tumor cell lines as well as to mesenchymal stem cells. As a result, miR-203 revealed a significant down-regulation in type 1 translocated ES cell lines whereas leukemia, osteosarcoma and neuroblastoma cell lines showed heterogeneous expression levels (see figure 5).

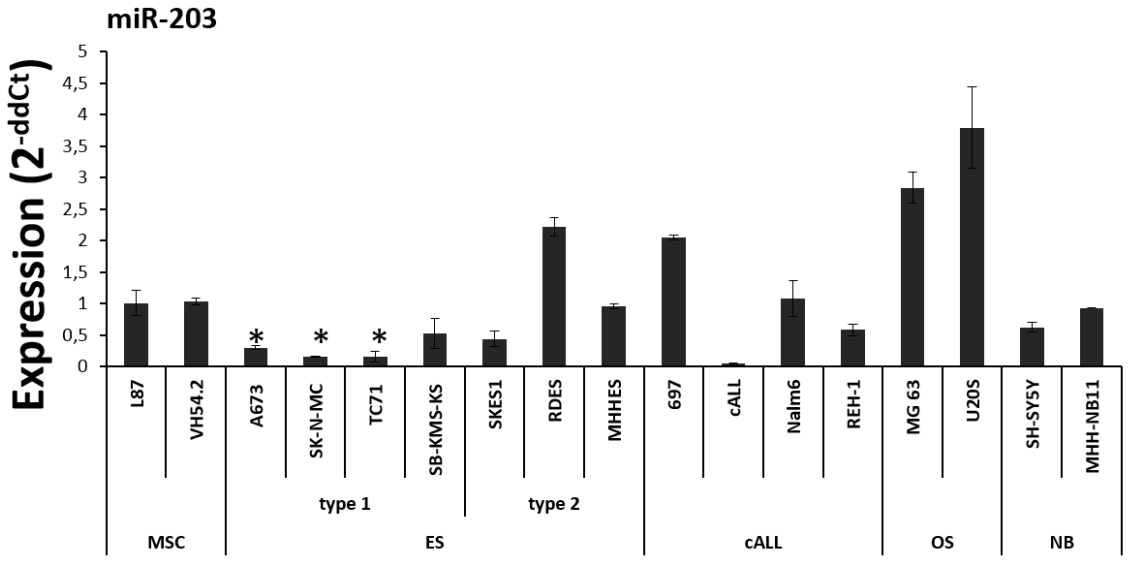

Figure 5: Expression of miR-203 on mRNA level in different ES cell lines. qRT-PCR data indicates miR-203 expression level in ES cell lines as well as in leukemia (cALL), osteosarcoma (OS) and neuroblastoma (NB) cell lines compared to mesenchymal stem cells. Data are mean ± SD; unpaired t-test (*$p < 0.05$)

4.3.2 miR-203 expression increases after EZH2 knock down

In order to identify regulatory mechanisms and verify possible epigenetic regulation of miR-203, EZH2 was knocked down in two different ES cell lines and expression changes were subsequently determined by qRT-PCR. For the knock down of EZH2, two different methods were chosen. The first was a transient knock down using RNA interference (RNAi) with specific siRNAs while the second was a constitutive EZH2 knock down (EZH2 pSIREN). This gene knock down was mediated by consistent expression of small hairpin RNAs (shRNA), which induced Dicer-dependent cleavage of endogenous EZH2 mRNA.

Using both methods EZH2 expression levels could be reduced to 20 – 40% residual expression. Transiently treated as well as constitutive cells revealed a 3-fold up-regulation of miR-203 after EZH2 knock down (see figure 6).

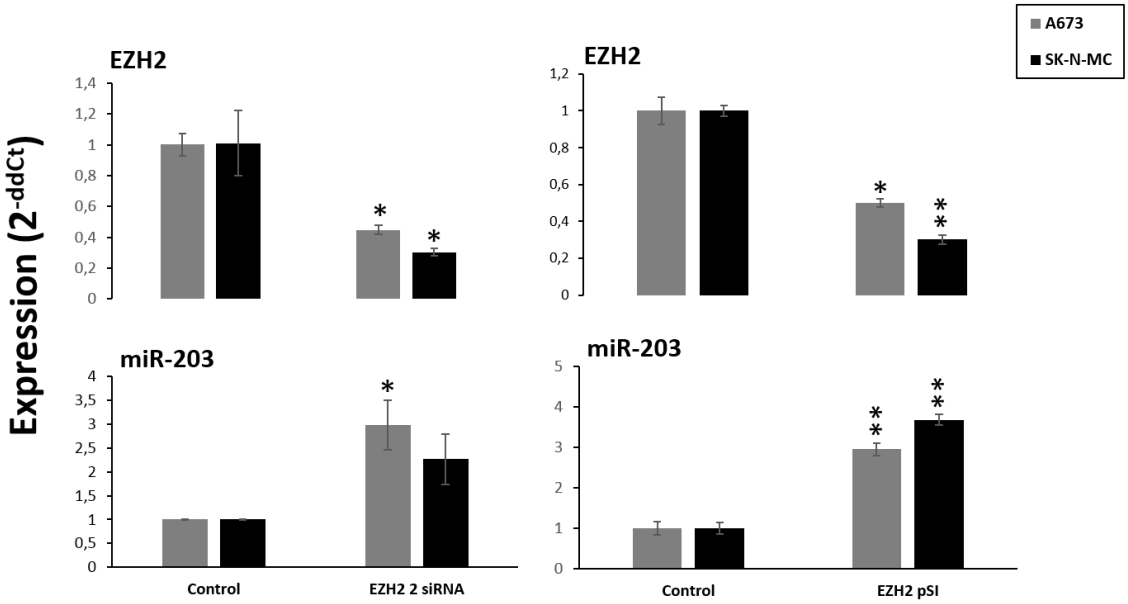

Figure 6: Up-regulation of miR-203 mRNA level after EZH2 knock down. Left panel: analysis after transient RNA interference with EZH2 2 siRNA for 72 h, compared to non-silencing control siRNA. Right panel: analysis of constitutive EZH2 knock down cells EZH2 pSI compared to non-silencing control cells. Data are mean ± SD; unpaired t-test (*p < 0.05; **p < 0.005).

4.3.3 EZH2 and EWS/FLI1 are down-regulated after exogenous up-regulation of miR-203

To assess whether EZH2 expression is also influenced by miR-203 expression describing a possible feedback loop, A673 and SK-N-MC cells were treated with miR-203 mimic. Mimics are chemically synthesized double stranded miRNA molecules that are assembled into the RISC-complex and enhance the biological effect of the special miRNA.

After treatment with 5 nM miR-203 mimic for 72h, RNA was isolated and expression of miR-203 as well as EZH2 and EWS/FLI1 was analyzed. Herein, miR-203 expression levels strongly increased and confirmed the functionality of the mimic. Additionally, EZH2 as well as EWS/FLI1 revealed reduced expression levels of down to 60% compared to the control (see figure 7). Similar results for EZH2 as well as EWS-FLI1 expression in A673 or SK-N-MC cells were observed with constitutive expression of miR-203 (see figure 8).

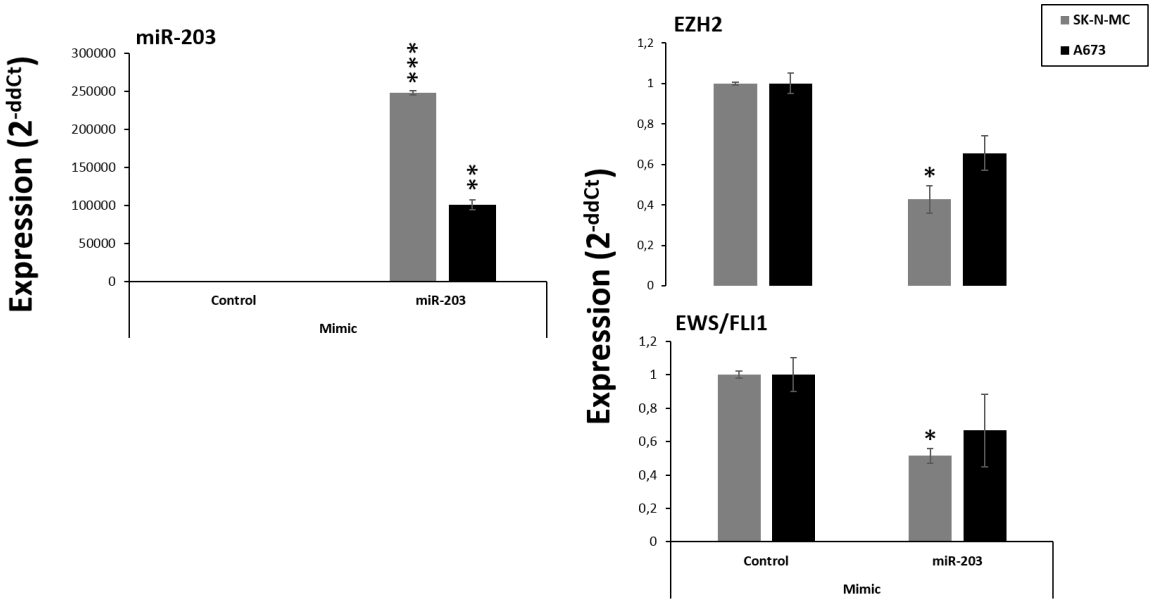

Figure 7: Influence of miR-203 on EZH2 and EWS-FLI1 after transient transfection with a mimic. Both cell lines A673 and SK-N-MC were treated transiently with a mimic for miR-203 and expression levels were analyzed using qRT-PCR. The negative control contained tumor medium and an equal amount of transfection reagent as the sample treated with mimic. Data are mean ± SD; unpaired t-test (*p < 0.05; **p < 0.005; ***p < 0.0005).

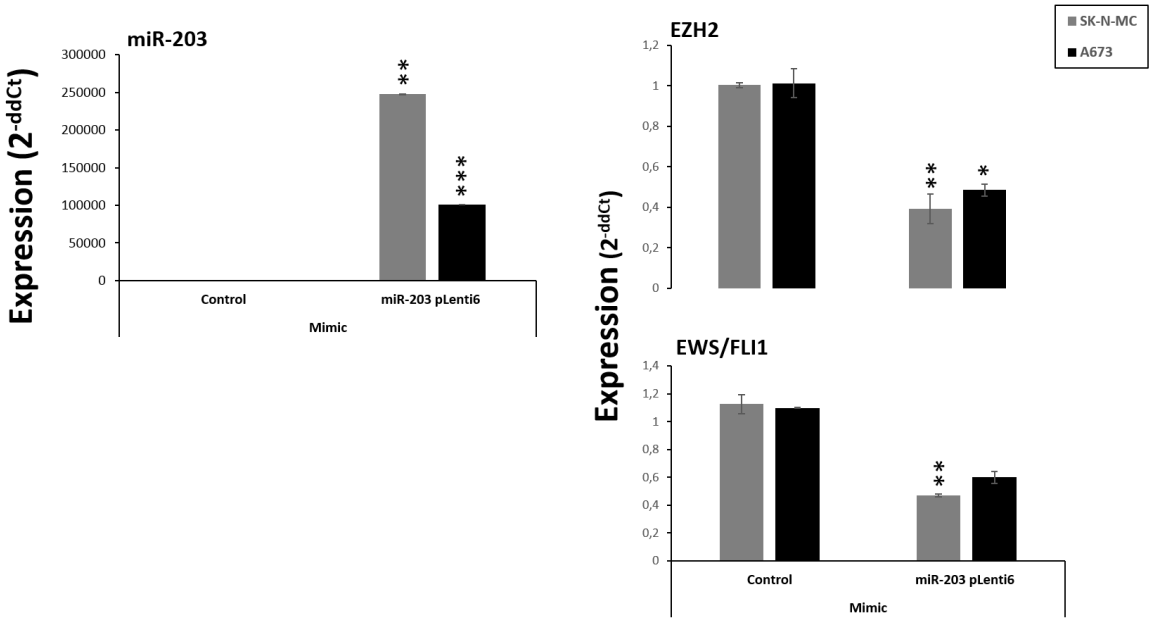

Figure 8: Influence of miR-203 on EZH2 and EWS/FLI1 after constitutive up-regulation. Cells with constitutive expression of miR-203 (miR-203 pLenti6) were generated (see 3.7) and subsequently, influence on EZH2 and EWS/FLI1 mRNA expression levels were analyzed using qRT-PCR. Data are mean ± SD; unpaired t-test (*p < 0.05; **p < 0.005; ***p < 0.0005).

4.3.4 Treatment with the EZH2 inhibitor GSK126 up-regulates miR-203 expression

In a next step, three ES cell lines were treated with an EZH2 inhibitor (GSK126). GSK126 binds specifically to the catalytic center of EZH2 and thus prevents the trimethylation of the lysine residue 27 of histone H3 (H3K27me3) whereby genes get reactivated. Thereby it is possible to examine the underlying epigenetic mechanisms regulating miR-203 expression (see 3.12.1).

By analyzing the qRT-PCR data an obvious up-regulation of miR-203 after inhibitor treatment for all three cell lines was depicted (see figure 10)**.** Additionally, a significant decrease of H3K27me3 levels was determined using western blot analysis further accompanied by an increase in H3 acetylation levels, a known mark of active transcription (see figure 9).

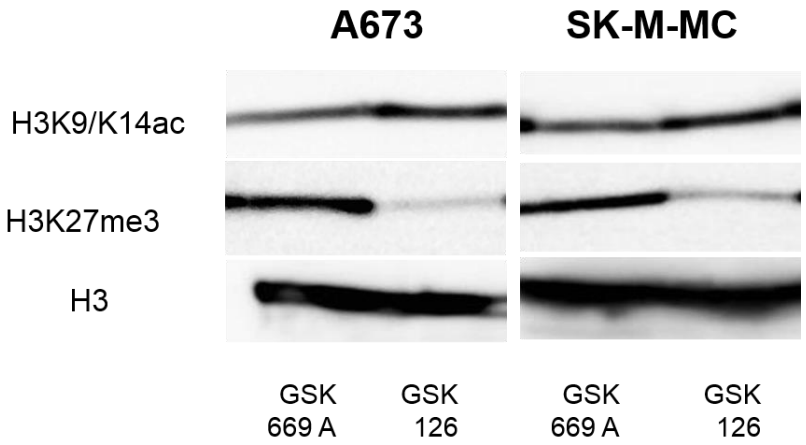

Figure 9: Western blot analysis detected modifications of H3 using specific antibodies. Detection of histone 3 (H3) protein amounts served as loading control, GSK669A served as negative control.

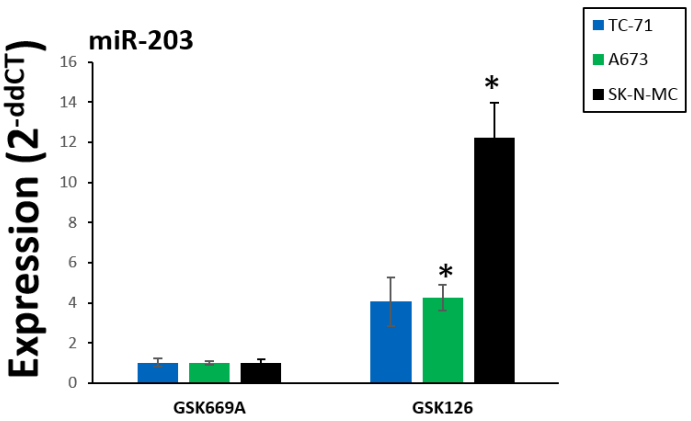

Figure 10: Strong up-regulation of miR-203 after treatment with the EZH2 inhibitor GSK126. A673, SK-N-MC and TC-71 were treated for 72 h, afterwards RNA was isolated and miRNA expression was determined using qRT-PCR. GSK669A treated cells served as negative control. Data are mean ± SD; unpaired t-test (*$p < 0.05$).

4.3.5 Histone deacetylases inhibitors upregulate miR-203 expression

All of the previously used three cell lines were subsequently treated with two different histone deacetylases (HDACs) inhibitors (see 3.12.2). The first, Trichostatin A (TSA) is a pan-HDAC inhibitor that selectively inhibits class I and II histone deacetylases but not class III HDACs. The second, MS-275 also known as Etinostat preferentially inhibits HDAC 1 and HDAC 3 with a nearly threefold higher affinity for HDAC 3. The negative control contained tumor medium and an equal amount of DMSO as a solvent control.

As shown in figure 12 all three cell lines showed an increased expression of miR-203 after treatment for 48h.

Furthermore, western blot analysis confirmed a broad inhibition of H3 acetylation as analyzed by H3K9/K14 acetylation (see figure 11).

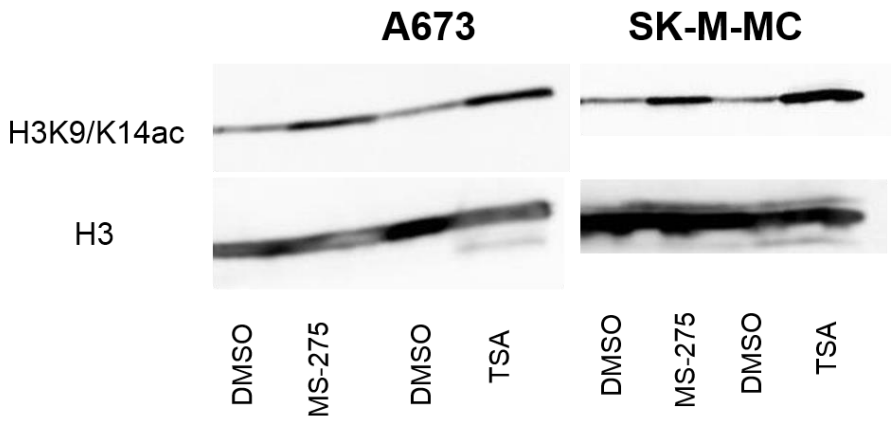

Figure 11: Western blot analysis detected modifications of H3 using specific antibodies. Detection of histone 3 (H3) protein amounts served as loading control**.**

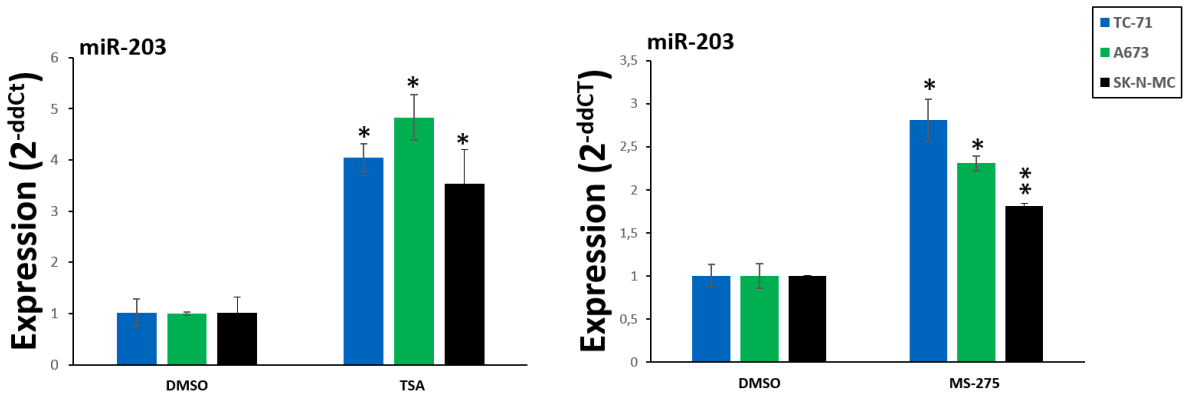

Figure 12: Expression of miR-203 after treatment with the HDAC inhibitors TSA and MS-275. A673, SK-N-MC and TC-71 were treated for 48 h, afterwards RNA was isolated and miRNA expression was determined using qRT-PCR. The negative control contained tumor medium and an equal amount of DMSO as the samples treated with the inhibitors. Data are mean ± SD; unpaired t-test (*p < 0.05; **p < 0.005).

4.3.6 Treatment with the DNA-methylation inhibitor 5-Aza-Cytidine (5-AzaC) up-regulates miR-203 expression likewise

Constitutive DNA-methylation possibly influencing miR-203 expression was further assessed by treating all three cell lines with 5-Aza-Cytidine. This inhibitor is an analogue of cytidine and prevents DNA methylation.

After treatment for 72h, RNA was isolated and analyzed by qRT-PCR. This treatment clearly demonstrated an up-regulation of miR-203 expression levels (see figure 13).

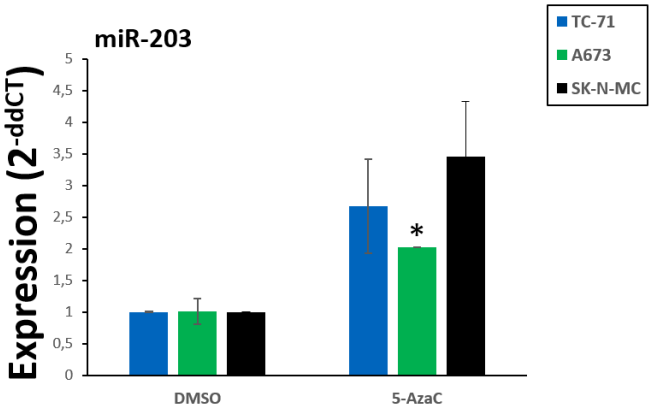

Figure 13: Up-regulation of miR-203 after treatment with 2 µM of DNA methylation inhibitor 5-AzaC. A673, SK-N-MC and TC-71 were treated for 72 h, afterwards RNA was isolated and miRNA expression was determined using qRT-PCR. The negative control contained tumor medium and an equal amount of DMSO as the samples treated with the inhibitors. Data are mean ± SD; unpaired t-test (*p < 0.05).

4.3.7 Overexpression of miR-203 reduces invasiveness *in vitro*

To further elucidate the role of miR-203 in ES oncogenesis, several *in vitro* assays were performed to monitor changes in biological characteristics after artificial up-regulation of miR-203. Invasiveness of the treated cells was measured by culturing them on Matrigel-covered plates for 48h (BioCoat™ Angiogenesis System*).* Subsequently, cells that had migrated through the membrane were stained with calcein and counted using fluorescence microscopy (see 3.9). As shown in figure 14 cells that have been treated with mimic for miR-203 revealed a considerably decreased invasive capacity of down to 20-30% in comparison to controls.

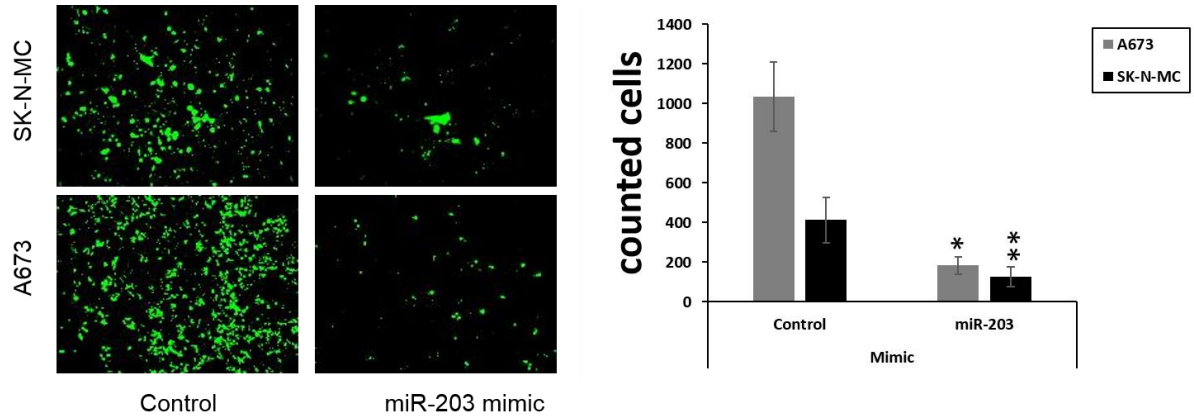

Figure 14: Analysis of invasiveness. A673 and SK-N-MC cell lines migrated through Matrigel after transfection with 5 nM of mimic for miR-203. The negative control contained tumor medium and an equal amount of transfection reagent as the sample treated with mimic Data are mean ± SD; unpaired t-test (*p < 0.05; **p < 0.005).

4.3.8 Overexpression of miR-203 inhibits contact independent growth *in vitro*

Furthermore, the effect of miR-203 up-regulation on contact independent growth was examined by performing colony formation assays using methylcellulose-based media (see 3.10). Therefore, ES cell lines A673 and SK-N-MC were seeded in duplicate and incubated for 14 days at 37°C in a humidified atmosphere (5% CO_2). Subsequently, the cells were photographed and formed colonies were counted. Thereby, up-regulation of miR-203 by transient mimic decreased the ability of tumor cells to grow contact-independently *in vitro*.

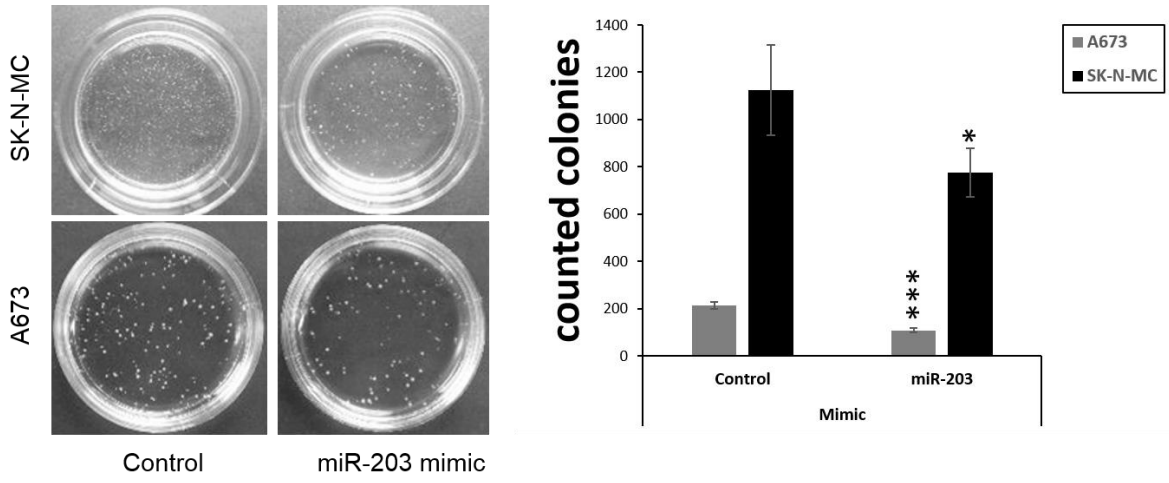

Figure 15: Colony formation assay. Contact independent growth of A673 and SK-N-MC cells after transient transfection with 5 nM mimic for miR-203. The negative control contained tumor medium and an equal amount of transfection reagent as the sample treated with mimic. Data are mean ± SD; unpaired t-test (*p < 0.05; ***p < 0.0005).

4.3.9 Overexpression of miR-203 reduces cell proliferation *in vitro*

The effect of miR-203 overexpression on cell proliferation was also measured in a contact dependent growth assay for A673 and SK-N-MC. Therefore, cells were seeded into special E-plates (see 3.8) and cultured for maximum of 168h. Treated cells showed a lower proliferation rate and also grew slower in both cell lines either with transient or constitutive miR-203 overexpression. Whereas, the effect was more significant for the transiently treated cells then for those with constitutive miR-203 expression.

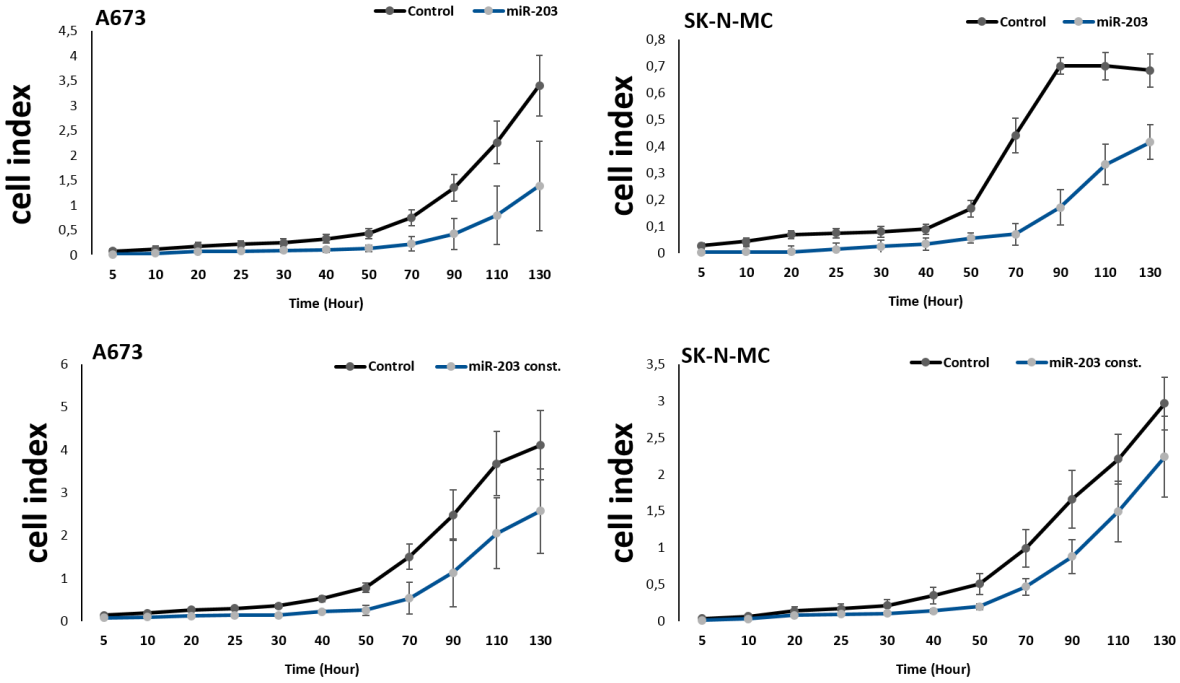

Figure 16: Proliferation Assay of A673 and SK-N-MC cells. Transiently transfected (upper panel) and constitutive (lower panel) miR-203 overexpression. Cellular impedance was measured every hour (relative cell index). Data are mean ± SD

To analyze whether the overexpression of miR-203 had an influence on cell cycle progression, A673 and SK-N-MC cells with transient mimic were tested using flow cytometry (see 3.11). Even though there was a difference in proliferation of treated cells as seen in the xCELLigence assay, cell cycle analysis could not reveal any changes in cell cycle progression.

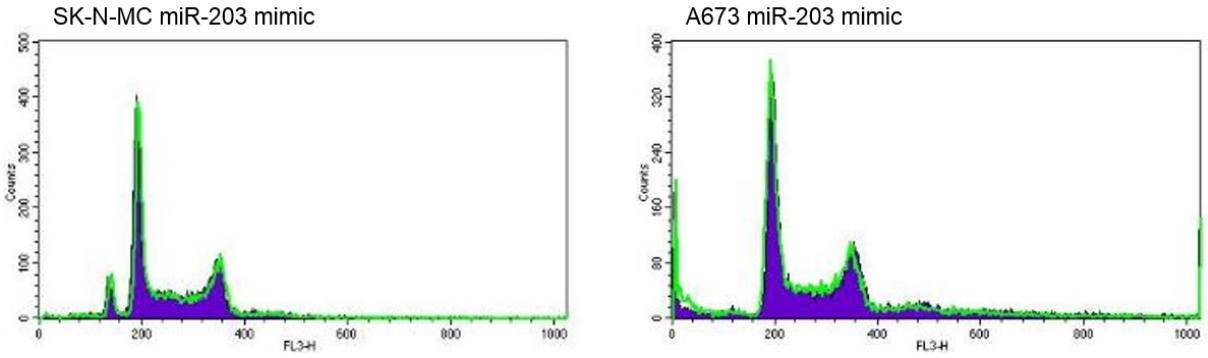

Figure 17: Cell cycle analysis. A673 and SK-N-MC cells with transient miR-203 overexpression. No differences between the treated cells (blue area) and the control (green line).

4.3.10. miR-203 overexpression does not affect tumor growth and metastatic spread *in vivo*

To find out whether the miR-203 overexpression affects tumor growth *in vivo*, A673 cells stably expressing miR-203 were injected subcutaneously into the inguinal region of immunodeficient mice and tumor growth was analyzed by survival (see 3.14). Unfortunately, as shown in figure 18 there was no delay of local tumor growth *in vivo*. Control mice as well as mice carrying overexpressed miR-203 cells had to be sacrificed concomitantly. miRNA expression analysis of post ex vivo tumor samples still showed high miR-203 levels confirming the well working overexpression.

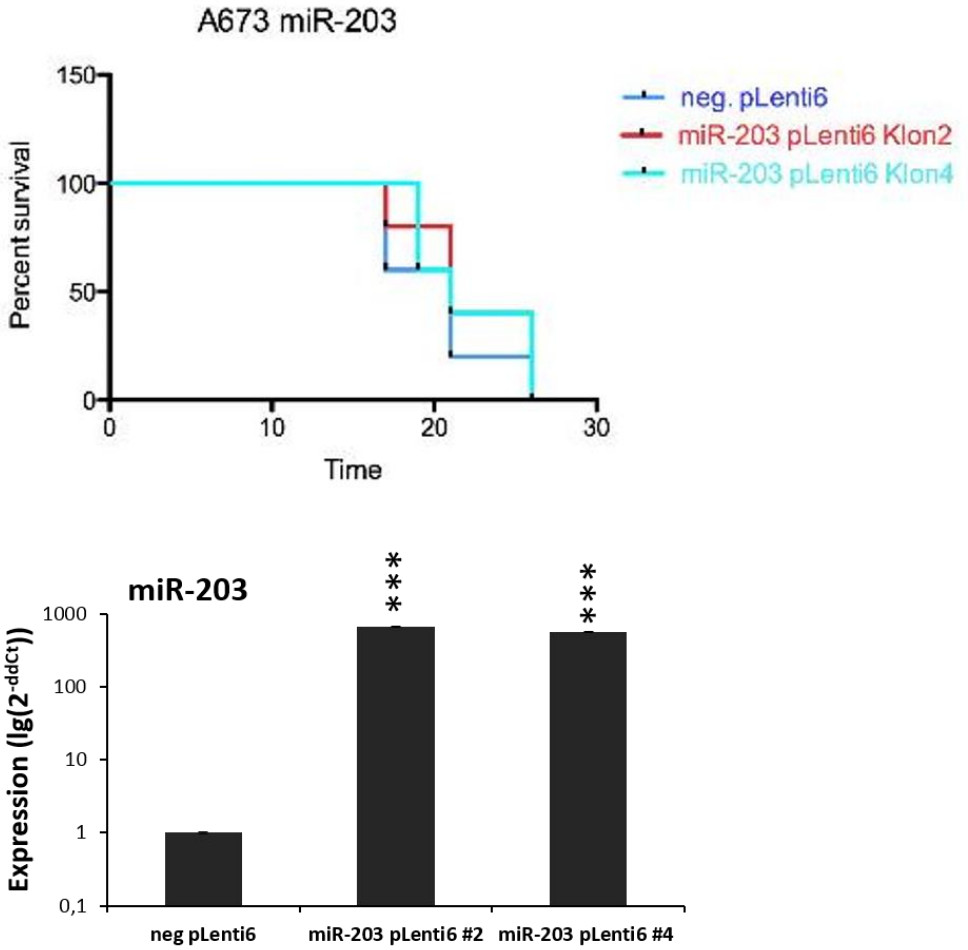

Figure 18: Local tumor growth *in vivo.* Upper panel: Kaplan-Maier survival curve. Evaluation of tumorigenicity of constitutive A673 miR-203 cells (miR-203 pLenti6) and appropriate negative control in immunodeficient mice (5 mice/group). Mice with an average tumor volume > 1 cm^3 were considered as positive and sacrificed.
Lower panel: Quantification miR-203 mRNA levels of tumor samples post ex vivo using qRT-PCR. Data are mean ± SD; unpaired t-test (***p < 0.0005).

Even though local tumor growth did not seem to be influenced we speculated based on results of in vitro invasiveness that tumor spread might be compromised by miR-203 over expression. Therefore, we injected A673 and SK-N-MC cells stably expressing miR-203 intravenously into the tail vein of mice and analyzed their metastatic spread. However, by counting metastases in liver or lung there was no significant difference measurable as shown in figure 19.

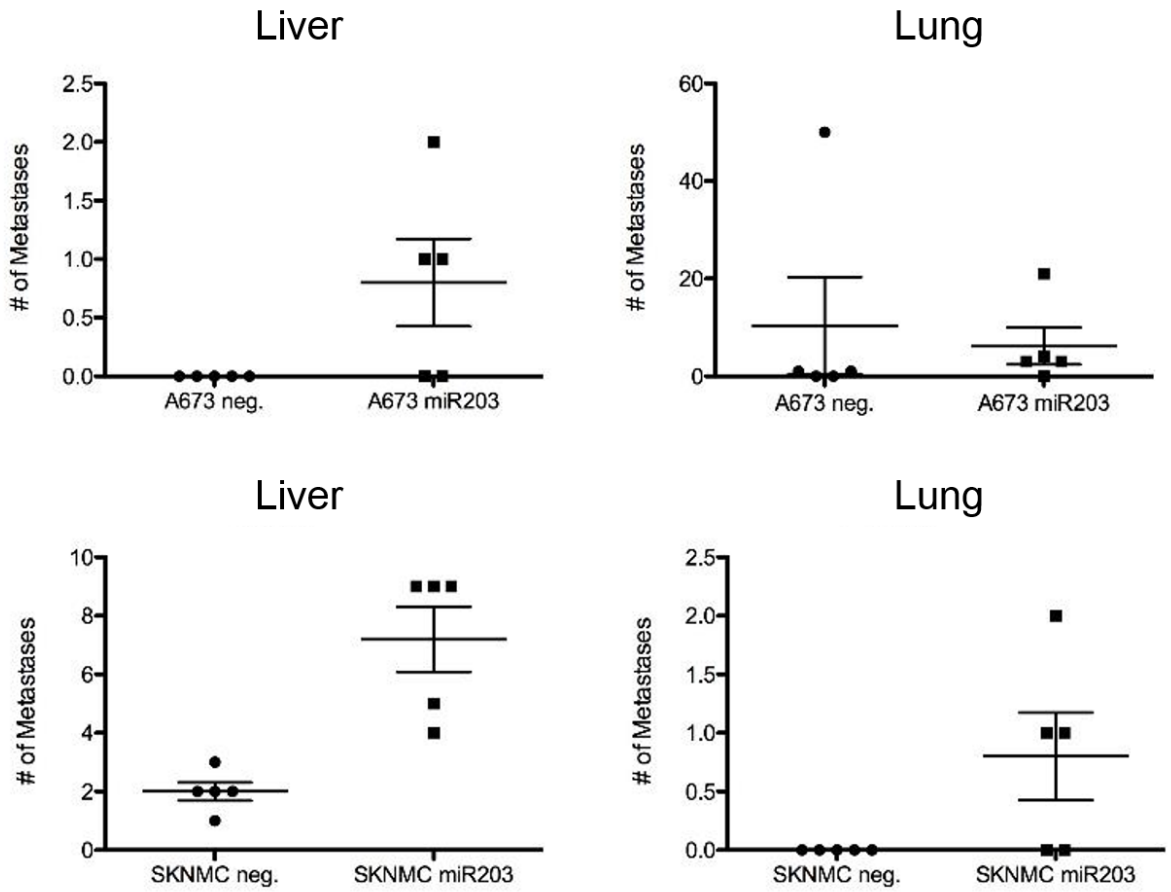

Figure 19: Metastatic potential *in vivo*. Cells with constitutive miR-203 expression were injected intravenously into the tail vein of mice. All macroscopically visible metastases in lungs and livers were counted. An average number of apparent metastases per mouse is shown.

4.4 The role of miR-497 in Ewing Sarcoma pathogenesis

4.4.1 miR-497 is overexpressed in primary ES cell lines

Similar to miR-203 an ES specific expression profile for miR-497 was established including several ES cell lines, other pediatric tumor cell lines as well as mesenchymal stem cell lines. Herein, miR-497 was found as up to 7-fold overexpressed in all primary ES cell lines.

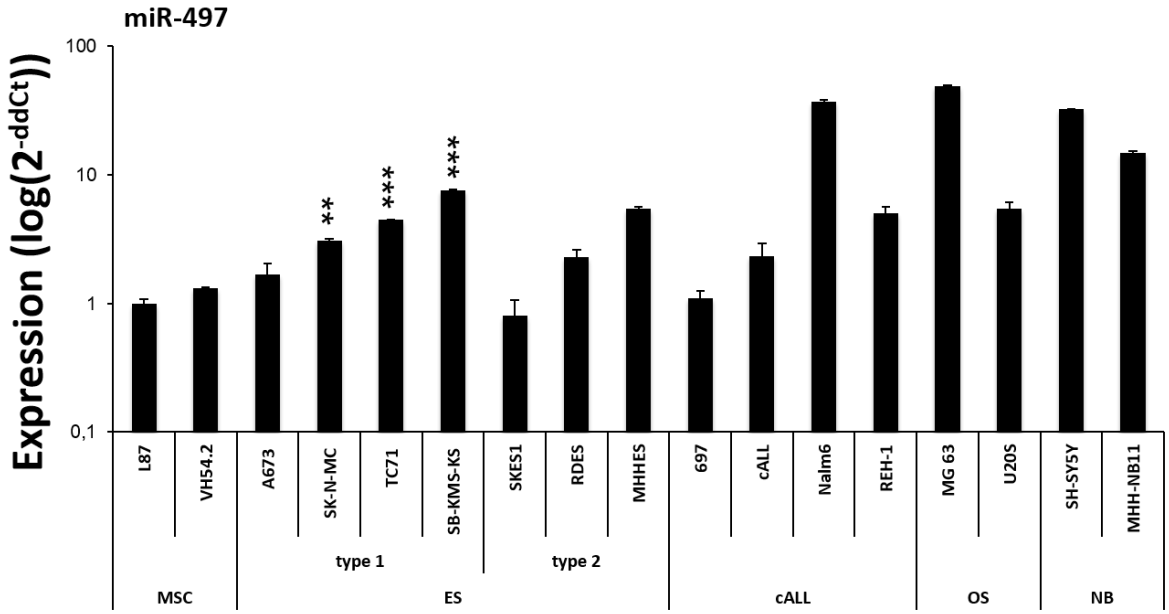

Figure 20: Expression of miR-497 on mRNA level in different ES cell lines. qRT-PCR data indicates miR-497 expression level in ES cell lines as well as in leukemia (cALL), osteosarcoma (OS) and neuroblastoma (NB) cell lines compared to mesenchymal stem cells. Data are mean ± SD; unpaired t-test (**p < 0.005; ***p < 0.0005).

4.4.2 miR-497 is down-regulated after EZH2 knock down

Possible interactive mechanisms between miR-497 and EZH2 regulating miR-497 expression were analyzed after EZH2 knock down in two different ES cell lines. Subsequently, miR-497 expression level was determined using qRT-PCR.

Using again a transient and a constitutive EZH2 knock down approach, EZH2 expression levels could be reduced down to 20 – 40% of residual expression. The transiently treated as well as the constitutive cells showed a significant down-regulation of miR-497 down to approximate 60%.

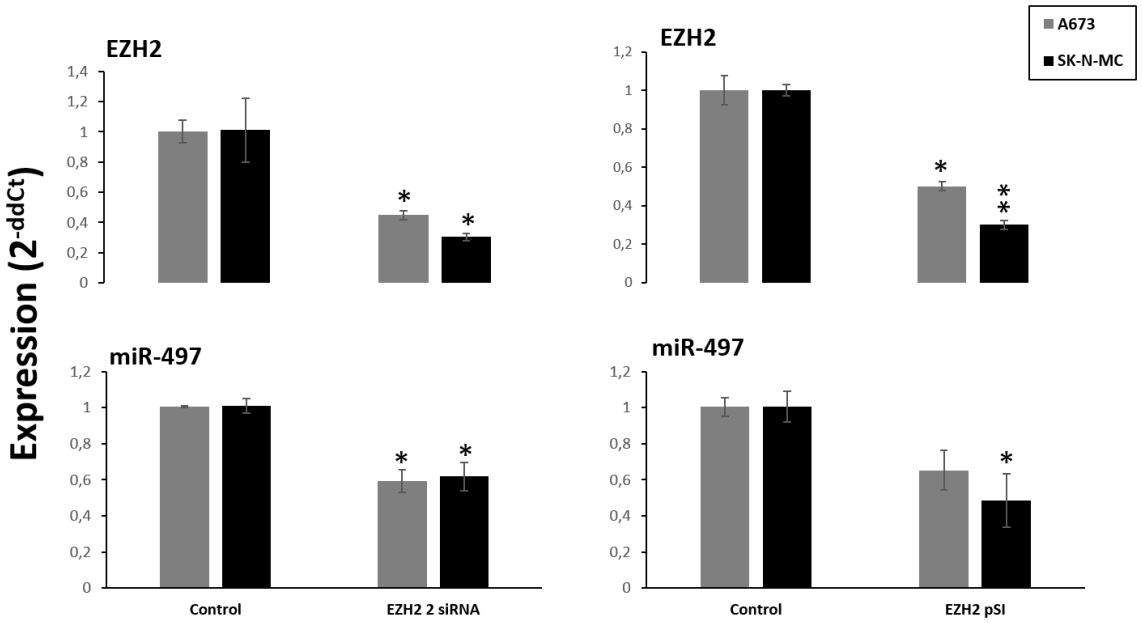

Figure 21: Down-regulation of miR-497 mRNA level after EZH2 knock down. Left panel: analysis after transient RNA interference with EZH2 2 siRNA for 72 h, compared to non-silencing control siRNA. Right panel: analysis of constitutive EZH2 knock down cells EZH2 pSI compared to non-silencing control cells. Data are mean ± SD; unpaired t-test (*p < 0.05; **p < 0.005).

4.4.3 EZH2 and EWS-FLI1 are likewise down-regulated after treatment with an specific inhibitor for miR-497

Considering the overexpression of miR-497 in ES cell lines the next step was to treat cells with an inhibitor specific for miR-497. After transient transfection for 72h with 50 nM of the inhibitor, RNA was isolated and the knock down of miR-497 as well as influences on EZH2 and EWS-FLI1 expression were analyzed by qRT-PCR. miR-497 showed decreased expression levels with less than 30% residual expression and confirmed the function of the inhibitor. Additionally, EZH2 as well as EWS/FLI1 revealed a reduced mRNA expression down to 20 – 60% (see figure 22).

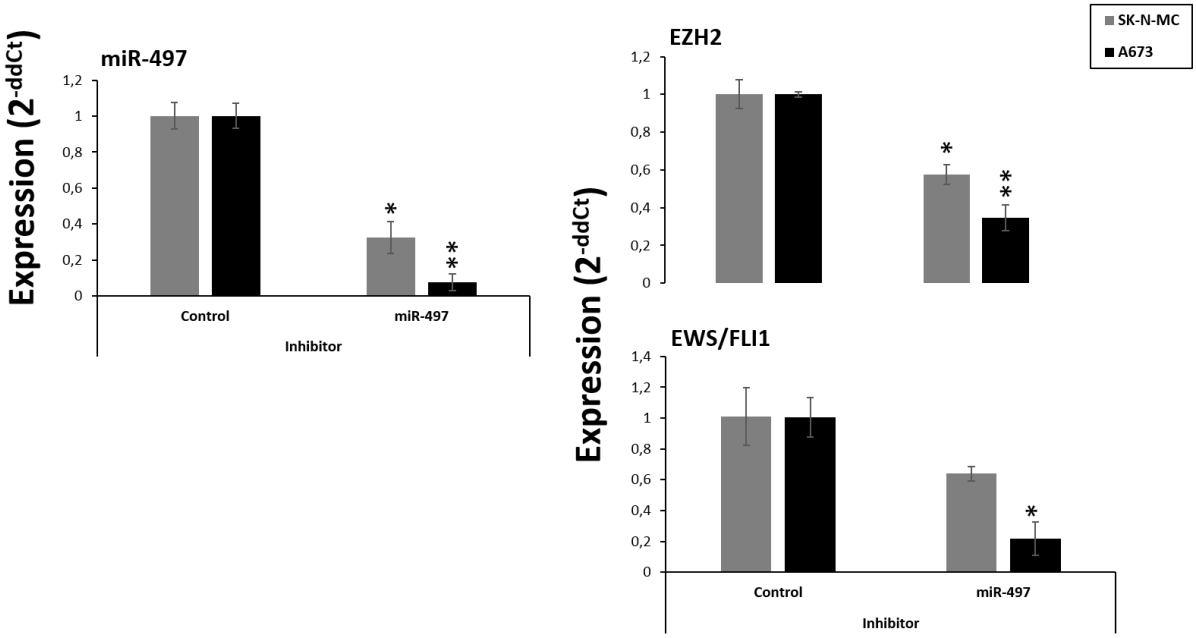

Figure 22: Influence of miR-497 on EZH2 and EWS/FLI1 after transient transfection with an inhibitor. Both cell lines A673 and SK-N-MC were treated transiently with an inhibitor for miR-497 and expression levels were analyzed using qRT-PCR. The negative control contained tumor medium and an equal amount of transfection reagent as the sample treated with inhibitor. Data are mean ± SD; unpaired t-test (*p < 0.05; **p < 0.005).

4.4.4 Treatment with the EZH2 inhibitor GSK126 leads to a down-regulation of miR-497

To shed further light on how miR-497 is regulated, A673, SK-N-MC and TC-71 were equally treated with 2 µM of the EZH2 inhibitor GSK126. In contrast to the results obtained for miR-203, qRT-PCR data revealed a decreased level of miR-497 after inhibitor treatment in all three cell lines (see figure 23).

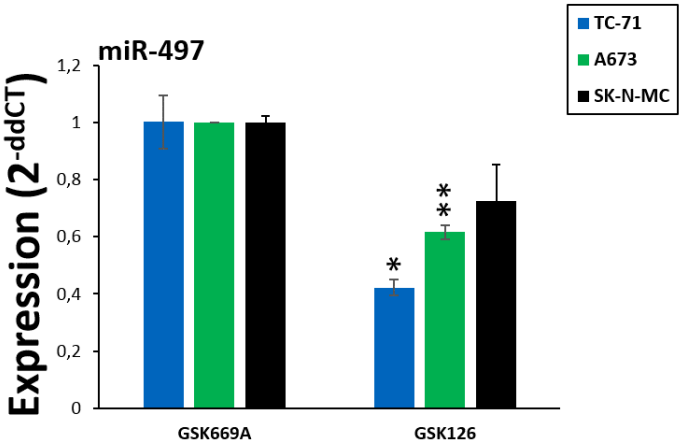

Figure 23: Down-regulation of miR-497 after treatment with the EZH2 inhibitor GSK126. A673, SK-N-MC and TC-71 were treated for 72 h, afterwards RNA was isolated and miRNA expression was determined using qRT-PCR. GSK669A treated cells served as negative control. Data are mean ± SD; unpaired t-test (*p < 0.05; **p < 0.005).

4.4.5 Up-regulation of miR-497 after treatment with the two HDAC inhibitors TSA and MS-275

A possible regulation of miR-497 through HDACs was assessed by treating cells with either 100 nM of TSA or MS-275 for 24h. In case of miR-497, the two inhibitors increased the expression levels as shown in figure 24, whereas MS-275 showed a stronger influence on the miRNA level.

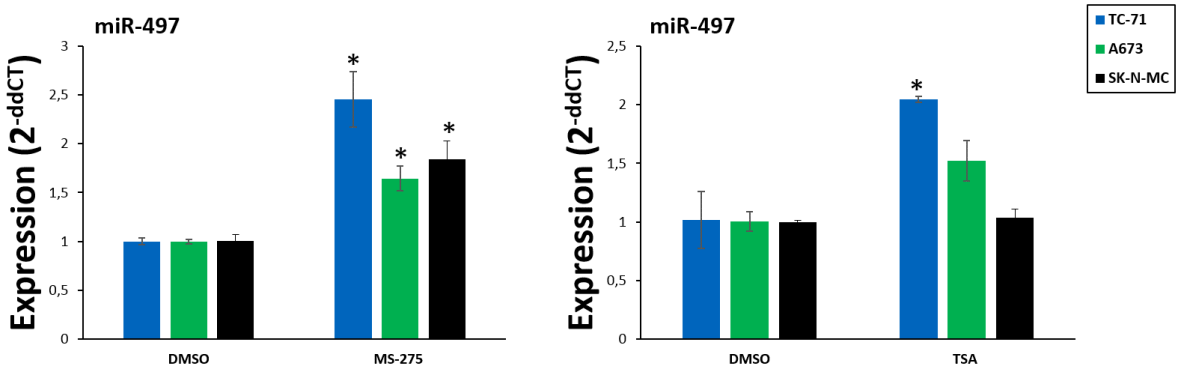

Figure 24: Expression of miR-497 after treatment with the HDAC inhibitors TSA and MS-275. A673, SK-N-MC and TC-71 were treated for 48 h, afterwards RNA was isolated and miRNA expression was determined using qRT-PCR. The negative control contained tumor medium and an equal amount of DMSO as the samples treated with the inhibitors. Data are mean ± SD; unpaired t-test (*p < 0.05).

4.4.6 Inhibition of mir-497 influences invasiveness *in vitro*

To elucidate the role of miR-497 in ES oncogenesis different *in vitro* assays have been conducted to analyze the changes after specific down-regulation of this miRNA, just as done for miR-203. The first step was to determine the influence on invasiveness. As shown in figure 25 cells with repressed miR-497 expression revealed a decreased invasive capacity.

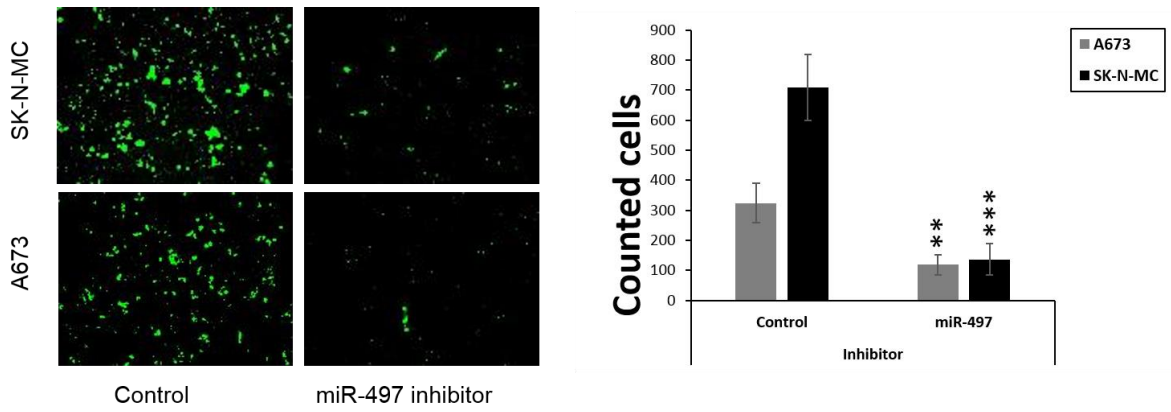

Figure 25: Analysis of invasiveness. A673 and SK-N-MC cell lines migrated through Matrigel after transfection with 50 nM of inhibitor for miR-497. The negative control contained tumor medium and an equal amount of transfection reagent as the sample treated with mimic Data are mean ± SD; unpaired t-test (**p < 0.005; ***p < 0.0005).

4.4.7 Inhibition of miR-497 has no influence on contact independent growth and cell proliferation *in vitro*

The observation of contact independent growth *in vitro* allows to make a prediction of the degree of malignancy of tumor cells. Hence, colony forming assay using methylcellulose-based media was performed. Unfortunately, the down-regulation of miR-497 showed no significant influence on contact independent growth capacity.

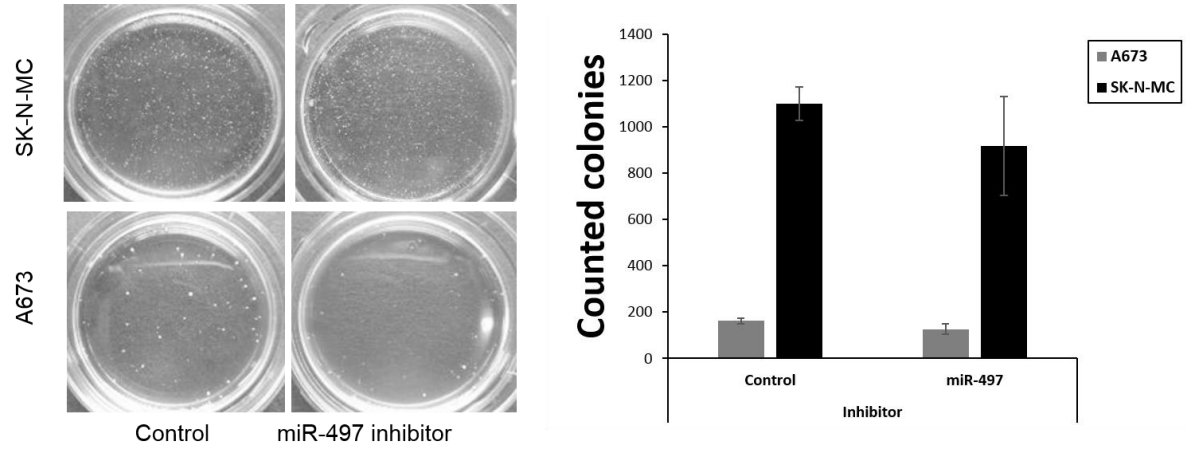

Figure 26: Colony formation assay. Contact independent growth of A673 and SK-N-MC cells after transient transfection with 50 nM inhibitor for miR-497. The negative control contained tumor medium and an equal amount of transfection reagent as the sample treated with mimic. Data are mean ± SD; unpaired t-test.

Additionally, the proliferative ability of the treated cells was evaluated using the xCELLigence proliferation assay. Similar to results of the colony forming assay no significant differences could be observed between treated and control cells (data not shown).

4.5 The role of miR-221 in Ewing Sarcoma pathogenesis

4.5.1 Intermediate expression of miR-221 in primary ES cell lines

miR-221 was analyzed by qRT-PCR and its expression compared to leukemia, osteosarcoma, neuroblastoma as well as MSCs. Therefore, miR-221 showed an intermediate expression level in ES cell lines that was not significantly up- or down-regulated.

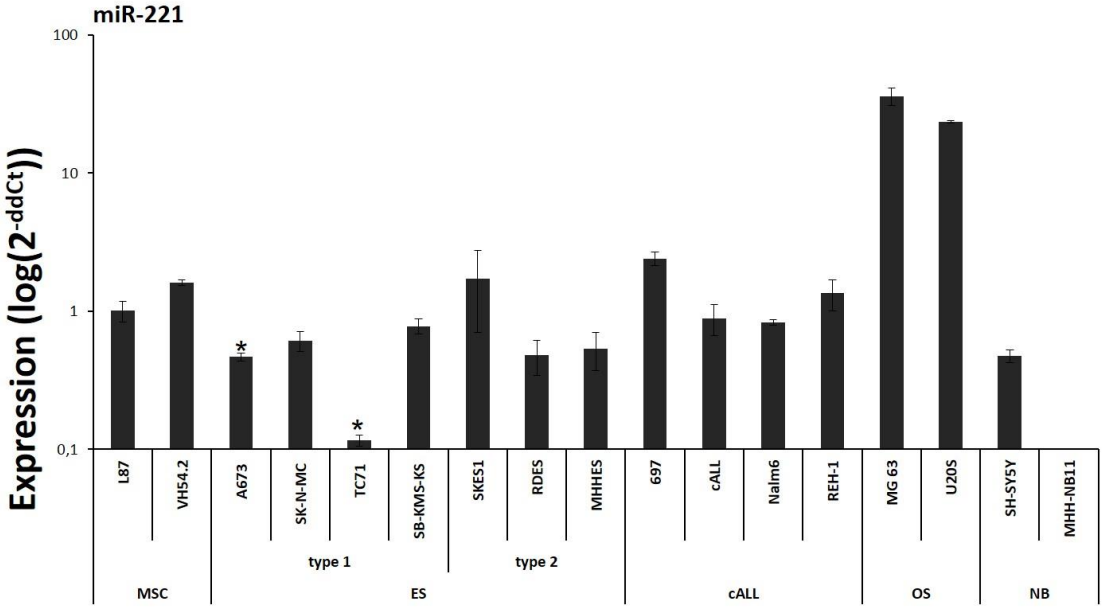

Figure 27: Expression of miR-221 on mRNA level in different ES cell lines. qRT-PCR data indicates miR-221 expression level in ES cell lines as well as in leukemia (cALL), osteosarcoma (OS) and neuroblastoma (NB) cell lines compared to mesenchymal stem cells. Data are mean ± SD; unpaired t-test (*$p < 0.05$).

4.5.2 Neither overexpression nor inhibition of miR-221 showed significant impact on EZH2 or EWS/FLI1 expression

In contrast to previous observations made by the group of T.J. Triché which reported miRNA-221 to be highly expressed in primary ES (Triché, 2008) our results revealed only an intermediate expression level without any significant up- or down-regulation. Regardless of this we treated our cells with 5 nM mimic and additionally with 50 nM inhibitor specific to miR-221 to evaluate possible effects on cell growth or invasiveness.

After 72h of treatment, RNA was isolated and qRT-PCR performed. The mimic as well as the inhibitor were indicated to be functional but in contrast to the results obtained for miR-203 or miR-497 neither the down-regulation nor the up-regulation of miR-221 had any consistent influences on EZH2 or EWS/FLI1 mRNA level. As shown in figure 28 up-regulation of miR-221 affected EWS/FLI1 expression most significant and doubled its expression in both cell lines.

The inhibitor however only showed a slight down-regulation of EZH2 up to 70 % residual expression (see figure 29).

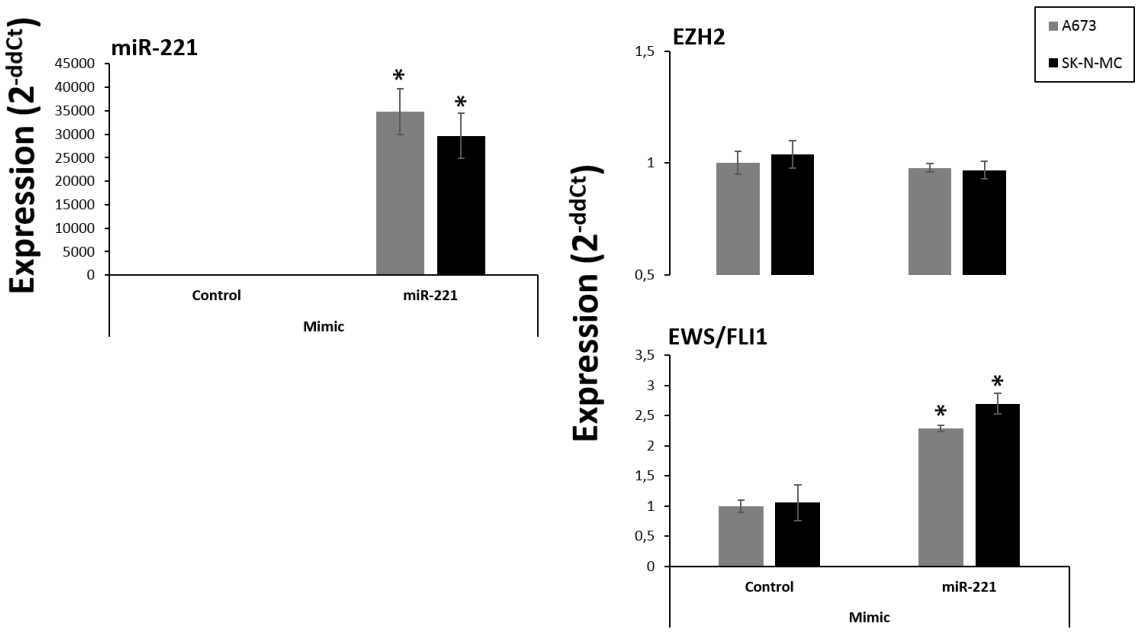

Figure 28: Influence of miR-221 on EZH2 and EWS/FLI1 after transient transfection with a mimic. Both cell lines A673 and SK-N-MC were treated transiently with a mimic for miR-221 and expression levels were analyzed using qRT-PCR. The negative control contained tumor medium and an equal amount of transfection reagent as the sample treated with mimic. Data are mean ± SD; unpaired t-test (*p < 0.05).

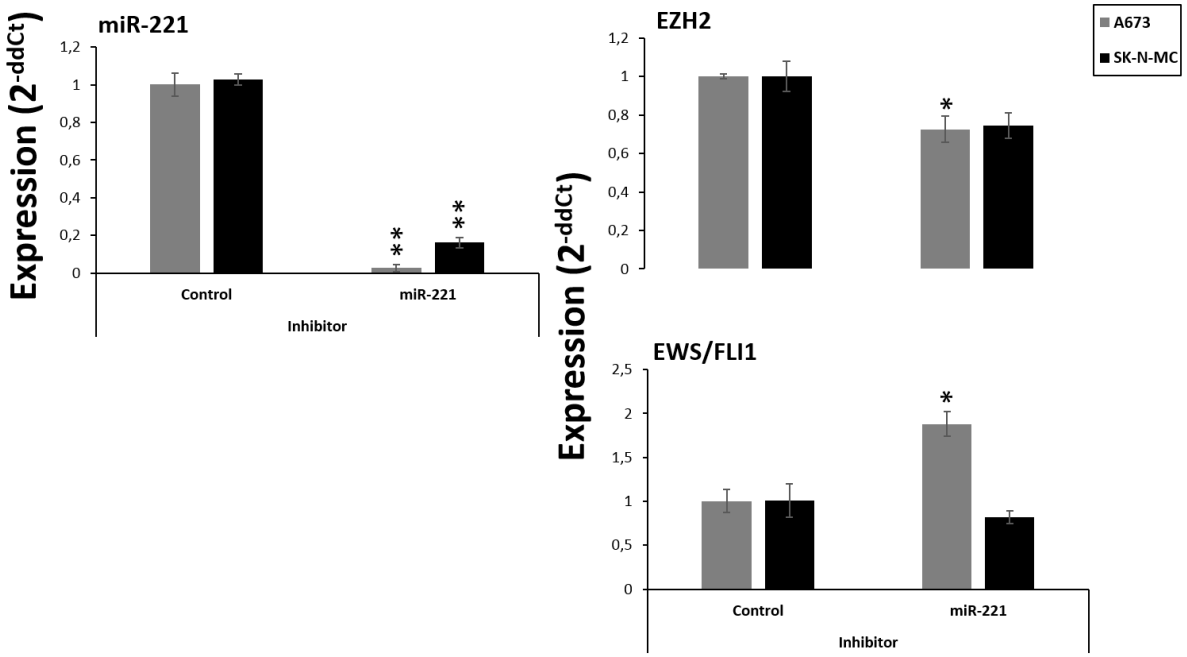

Figure 29: Influence of miR-221 on EZH2 and EWS/FLI1 after transient transfection with an inhibitor. Both cell lines A673 and SK-N-MC were treated transiently with an inhibitor for miR-221 and expression levels were analyzed using qRT-PCR. The negative control contained tumor medium and an equal amount of transfection reagent as the sample treated with mimic. Data are mean ± SD; unpaired t-test (*p < 0.05; **p<0.005).

4.5.3 miR-221 showed no significant changes after epigenetic inhibition

miR-221 was also examined for alterations on the epigenetic level. However, miR-221 revealed no significant changes after treatment with the different inhibitors. Neither GSK126 nor 5-AzaC or HDAC inhibition by TSA or MS-275 influenced mRNA expression levels significantly. Additionally, EZH2 knock down did not modify miR-221 either (data not shown).

4.5.4 Inhibition as well as overexpression of miR-221 influences invasiveness *in vitro*

Despite of these controversial results the relevance of miR-221 in ES oncogenesis was determined. Each assay was carried out for mimic as well as for inhibition of miR-221. In case of invasive growth cells with mimic as well as those with inhibition of miR-221 revealed less invasive capacity (see figure 30).

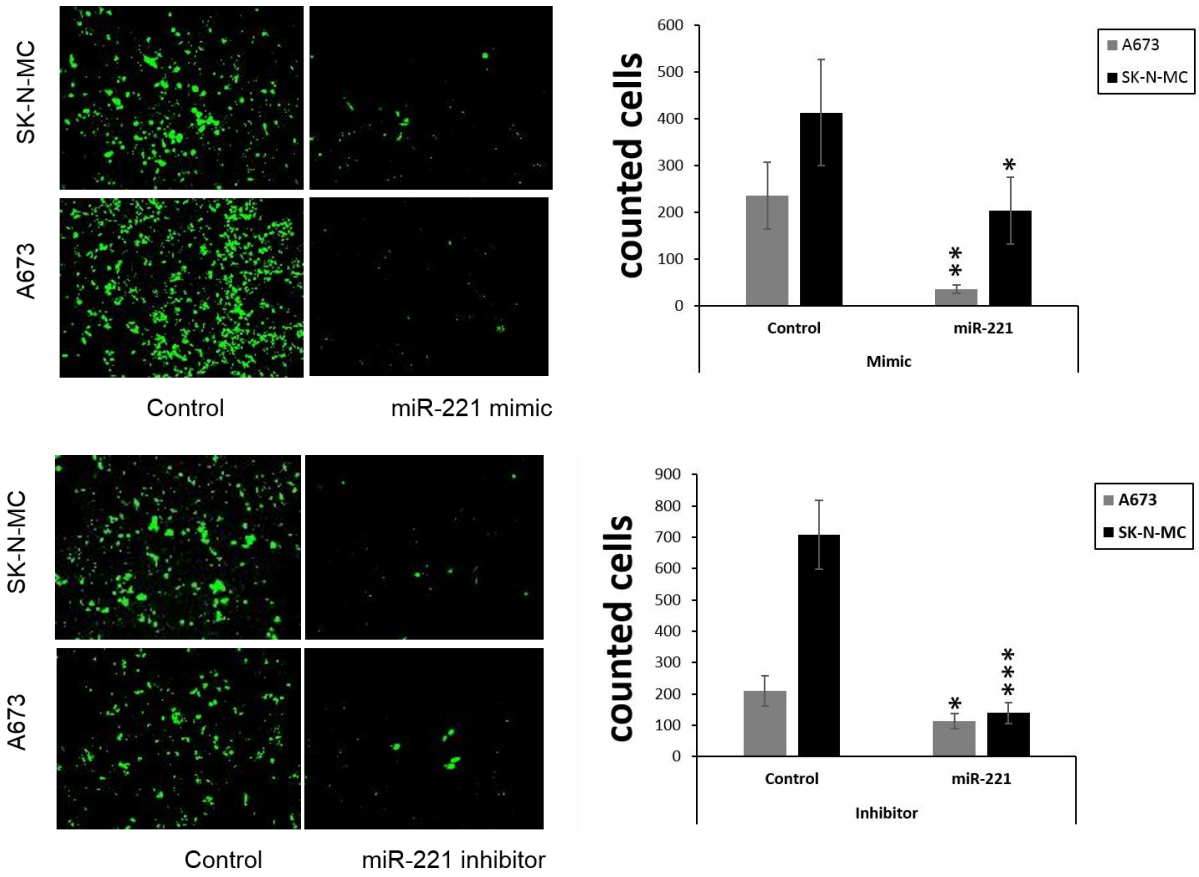

Figure 30: Analysis of invasiveness. A673 and SK-N-MC cell lines migrated through Matrigel after transfection with 5 nM of the mimic (upper panel) and 50 nM of inhibitor (lower panel) for miR-221. The negative control contained tumor medium and an equal amount of transfection reagent as the sample treated with mimic Data are mean ± SD; unpaired t-test (*p<0.05;**p<0.005; ***p < 0.0005).

4.5.5 Neither inhibition nor overexpression of miR-221 had an influence on contact independent growth and cell proliferation in vitro

In a final experiment, miR-221 was also analyzed for contact independent growth using colony formation assay as well as for its proliferating capacity. However, neither inhibition nor overexpression of miR-221 influenced the ability to grow in methylcellulose-based media (data not shown).

Furthermore, the proliferation assay revealed no relevant differences of proliferation capacity after inhibition or overexpression of miR-221 in both cell lines, A673 and SK-N-MC (data not shown).

4.6 Schematic summary of obtained results

TABLE 22: SUMMARY OF RESULTS

	miR-203	**miR-221**	**miR-497**
Expression ES/MSC	Down regulated	Intermediate level	Up regulated
EZH2 siRNA	Up regulated	No change	Down regulated
EZH2 inhibitor (GSK126)	Up regulated	No change	Down regulated
5 AzaC	Up regulated	No change	No change
HDAC inhibitor (TSA/MS-275)	Up regulated	No change	Up regulated
Mimic: measure EZH2/EWS-FLI1	Down regulated	No change	———
Inhibitor: measure EZH2/EWS-FLI1	———	No change	Down regulated

5. Discussion

5.1 The role of miR-221 in ES pathogenesis

Different studies describe miR-221 to be over-expressed in cancer and to have an impact on tumor progression (Nassirpour, Mehta, Baxi, & Yin, 2013; Stinson et al., 2011; Visone et al., 2007). For example, in hepatocellular carcinoma over-expressed miR-221 directly promotes tumor growth by facilitating cell cycle progression (Fornari et al., 2008; Pineau et al., 2010). Equally, in hematopoetic malignancies as well as in prostate carcinoma miR-221 functions as a miRNA oncomir by manipulating cell cycle regulatory mechanisms (Frenquelli et al., 2010; Garzon et al., 2008). In all cases miR-221 inhibits cyclin-dependent kinase inhibitors or components who normally prevent cell cycle progression from G1 to S phase contributing to the development of an invasive and highly malignant phenotype. Furthermore, several studies were able to show that inhibition of miRNA-221 induces apoptosis and decreases tumor growth *in vivo* (Mercatelli et al., 2008; Park, Lee, Esau, & Schmittgen, 2009).

Intriguingly, all the different results indicated that miRNA expression levels are very distinct between different tumor entities and their biological functions are very specific and not necessarily transferable to different types of cancer. Even within one type of cancer contradictory functions may appear between different cell lines or tumors.

Plehm et al. as well as T.J. Triche reported miRNA-221 to be highly expressed in primary ES (Plehm, 2011; Triché, 2008). On the other hand, Mc Kinsey et al. were able to demonstrate that miR-221 expression is strongly repressed by EWS-FLI1 function, pursuing a miRNAs negative regulation of the expression of multiple pro-oncogenic components of the IGF pathway.(McKinsey et al., 2011).

These contradictory observations left us with the question how can those different results arise for one and the same tumor? This is why we first took a deeper look into how the miRNA was analyzed.

To determine miRNA expression, it is necessary to normalize data and thus adjust variabilities in miRNA and cDNA quantity to cellular and experimental variations. For this purpose housekeeping genes presumably constantly expressed need to be determined. There are two points possibly contributing to the above-named different results of mir-221 expression and function. First of all, different studies use different housekeeping genes. After the normalization with unequal reference genes study results are not completely comparable any

longer. For example, Plehm et al. used RNU19 for normalization. A non-coding RNA very frequently used in a broad range of different tumor entities. However, we found RNU19 to be influenced by our experimental conditions. Therefore, several possible housekeeping genes including RNU19, RNU6B and RNU48 were taken into account and analyzed under different treatment regimens. As a result, we found RNU48 to be most constantly expressed under all conditions tested and used this miRNA for all further analysis as our new housekeeping gene (see 4.2).

Furthermore, Gee et al. were able to demonstrate that commonly used housekeeping genes like RNU44, RNU48, RNU43 and RNU6B are not as constantly expressed as assumed. Even more, the study provides evidence that these small nucleolar RNAs (snoRNAS) are deregulated in cancer as well and thus may introduce certain biases (Gee et al., 2011).

When Plehm et al. examined miR-211 expression levels in ES they compared different ES cell lines only among each other and with other pediatric tumor cell lines. Meaning that they had no appropriate corresponding non-tumorigenic tissue as a reference cell line. In contrast, here we studied also mesenchymal stem cells (MSCs) as the considered cells of origin of ES. Therefore, all ES specific miRNA expression profiles were checked against MSCs as reference and other pediatric tumor cell lines (see figure 27).

As a consequence results of Plehm et al. could not be reproduced in this thesis. In our studies, miR-221 showed no significant deregulation in ES cell lines in contrast to MSCs.

Taking into account the different methods used, contradictory results from previous publications and the more intermediate expression level of miR-221 found in this study we decided to examine both influences.

Therefore, we treated cells with a mimic or with an inhibitor for miR-221 to detect possible alteration in tumor specific biological capacities. Unfortunately, none of the approaches revealed any significant influence on EZH2 or EWS-FLI1 expression levels (see figure 28 and 29). If at all, we observed some minor influence especially on EWS-FLI1. Also, the examination of epigenetic regulation processes possibly influencing miR-221 expression revealed no significant results. Apparently, the effects of miR-221 in ES depend if at all on other regulatory pathways different from EZH2 or histone modification. To shed further light on its role in ES future experiments should reconsider a possible dependence on EWS/FLI1 and its influence on cell cycle regulation as previously suggested (Galardi et al., 2007).

However, since further *in vitro* assays revealed no significant influence of miR-221 on biological properties of ES cell lines it should also be considered that this miRNA might not play an important role for ES pathogenesis.

5.2 The role of miR-497 in ES pathogenesis

miRNA-497 is a member of the miR-15 family and forms a cluster with miR-195. miRNAs of one cluster share the same pre-miRNA, they are transcribed by the same promotor and thus may be controlled by common regulatory elements. Consequently, cluster miRNAs have related physiological and pathophysiological functions (Kim et al., 2009; Mogilyansky & Rigoutsos, 2013). All studies analyzing these functions in detail revealed that miR-497 acts as a tumor suppressor. In hepatocellular carcinoma for example, miR-497 and miR-195 are likely to inhibit cell growth by suppressing cell cycle progression. Flow cytometry analysis showed significant accumulation in G0/G1 phase after transfection with a respective miRNA mimic (Furuta et al., 2013). In breast cancer, overexpression of miR-497 resulted in decreased mRNA and protein levels of BCL-2, a member of the apoptotic pathway. Thereby, miR-497 demonstrated to be able to suppress proliferation, initiate apoptosis and mediate cell cycle arrest in G0/G1 phase (Shen et al., 2012). Similar results were obtained by Ge et al. studying the influence of miR-497 on Osteosarcoma pathogenesis. They restored miR-497 expression and thereby successfully suppressed tumor growth *in vitro* and *in vivo* (Ge, Zheng, Li, Niu, & Li, 2016).

5.2.1 Connection between EZH2 and miR-497 in ES

This thesis demonstrated that miR-497 expression levels changed after EZH2 knock down. However, this time EZH2 knock down as well as its enzymatic inhibition by GSK126 resulted in a decreased expression of miR-497 (see figure 21 and 23). Therefore, EZH2 enhanced miR-497 expression which points to a so far unknown non-canonical function.

In addition, specific expression of miR-497 in ES did not behave as observed in other cancer entities. In this study, the expression of the miRNA compared to mesenchymal stem cells and other pediatric tumor cell lines showed a significant increase. Therefore, we used an antimir to specifically inhibit miRNA function and observed an EZH2 as well as EWS/FLI1 attenuated expression level.

Apparently, on the one hand miR-497 is influenced in a way by EZH2 and on the other hand the miRNA itself is able to modify EZH2 and EWS/FLI1 expression levels. Whether these processes directly interact or if there are additional regulatory mechanisms still need to be investigated.

5.2.2 Histone acetylation regulates miR-497 expression level

So far, only very little is known about the underlying epigenetic processes regulating miR-497 expression. In a first attempt Furuta et al. observed miR-497 to be down regulated in hepatocellular carcinoma at the transcriptional level rather than post-transcriptional. He further showed that down-regulation appeared already at the level of pri-miRNA procession (Furuta et al., 2013). To assess epigenetic mechanisms participating in the up-regulation of miR-497 in ES, three cell lines were treated with the different inhibitors targeting DNA methylation (5AzaC) or histone deacetylation (TSA and MS-275) (see figure 24). Suzuki et al. hypothesized based on a genome-wide analysis of mRNA expression, combined together with analysis of chromatin structure and DNA-methylation, miR-497 to be regulated by promoter-CpG island methylation in colorectal cancer (Suzuki et al., 2011). Similar observations could be made in breast cancer where a down-regulation of miR-497 was mediated by DNA-methylation (Li et al., 2011).

5-AzaC is a chemical analog of cytidine, a nucleoside that is a natural building block of DNA or RNA. Incorporation of 5-AzaC into DNA leads to an irreversible inhibition of DNA-methyltransferases (DNMT) and DNA methylation cannot take place resulting in the reactivation of previously silenced genes (Christman, 2002).

However, miR-497 expression in ES cell lines showed no significant changes after treatment with 5AzaC in this study (data not shown).

But, when treating ES cells with the two histone deacetylase (HDAC) inhibitors TSA and MS-275 an increased expression of miR-497 was observed. Especially MS-275, inhibiting only class I HDACs (HDAC1, 2 and 3) and the class II A HDAC9 had the strongest influence on miR-497 expression. Concluding that histone acetylation contributes to the up-regulation of miR-497 in ES. Still, it is unclear how exactly EZH2 and HDAC activity contribute to the up-regulation of miR-497 in ES. Further investigations should follow to clarify these underlining relations.

5.2.3 Inhibition of miR-497 reduces invasiveness *in vitro*

Although, all previous studies describe miR-497 to be down regulated in most cancer entities and to act as a tumor suppressor, we found miR-497 to be up regulated in ES. Therefore, we further considered miR-497 to have oncogenic potential in ES and assayed it in several *in vitro* assays analyzing its potential malignant influence. Surprisingly, only the analysis of its influence on invasiveness generated significant results. Inhibition of miR-497 using a specific antimir resulted in a decreased invasive capacity whereas it had no influence on contact independent growth or cell proliferation.

5.3 The role of miR-203 in ES pathogenesis

Over the last few years miR-203 emerged as an attractive tumor suppressor miRNA candidate in several different cancer entities. Thereby miR-203 could be shown to inactivate oncogenes that favor cell proliferation as well as the development of metastasis. In hematopoietic malignancies for example, miR-203 was described to regulate the oncogenic BCL-ABL1 axis. Up-regulation of miR-203 reduced the BCL-ABL1 fusion protein level and thereby cell proliferation ability (Bueno et al., 2008).

Furthermore, advanced prostate cancer with bone metastasis demonstrated attenuated miR-203 levels. The reintroduction of the miRNA in those cell lines led to a significantly reduced metastatic spread (Saini et al., 2011). Most recently, miR-203 was also shown to be down regulated in osteosarcoma, the most frequent bone cancer in children. Its artificial up-regulation in these tumors inhibited cell proliferation and migration (Yang, Liu, & Wang, 2015). However, even though there is ample evidence for the importance of miR-203 in different cancer entities the expression and role of miR-203 in ES has not been examined yet. In this study, miR-203 specific expression levels in ES were analyzed and compared to mesenchymal stem cells as well as to other pediatric tumor cells.

As a first result miR-203 revealed a significantly decreased expression in all type I ES cells (see figure 5) indicating a presumable mechanism that suppresses critical miRNAs like miR-203 to enhance tumorigenicity of ES.

5.3.1 Down-regulation of miR-203 in ES by DNA- hypermethylation

Since most studies revealed miR-203 to be epigenetically silenced by promotor hypermethylation, its re-expression resulted in restrained tumor cell proliferation, inhibited cell migration and better differentiation. In rhabdomyosarcoma as well as in hepatocellular carcinoma DNA-demethylating agents achieved reactivation of miR-203 expression (Diao et al., 2014; Furuta et al., 2010; Saini et al., 2011). After the treatment of ES cells with 5-AzaC expression of miR-203 demonstrated a significant up-regulation. Therefore and in concordance with results shown for other tumor entities (Kozaki, Imoto, Mogi, Omura, & Inazawa, 2008; Zhang et al., 2011) miR-203 expression is presumably in part silenced by DNA hypermethylation in ES.

5.3.2 miR-203 expression is regulated by EZH2

The ES specific dominant chromosomal translocation derived transcription factor EWS-FLI1 directly mediates a strong EZH2 overexpression and thus, contributes to enhanced tumorigenicity of ES (Richter et al., 2009).

Following EZH2 inhibition with transient knock down using specific siRNAs as well as after constitutive EZH2 knock down, a significant miR-203 up-regulation was observed. Comparable results emerged after treating ES cells with the enzymatic EZH2 inhibitor GSK126 wherein miR-203 became re-expressed. The gain of activity was demonstrated by an increased mRNA level in qRT-PCR as well as augmented H3 acetylation in western blot analysis indicating a close relationship between EZH2 activity and miR-203 expression.

Considering our results of miR-203 re-expression after inactivation of DNA-methylation, EZH2 itself seems to be able to influence DNA-methylation.

Already, embryonic stem cells undergo *de novo* DNA-methylation during the differentiation to more specialized precursors in the context of Polycomb complex mediated patterning during gastrulation. Similarly, cancer cells target de novo DNA-methylation by taking advantage of the pre-existing PRC2-mediated epigenetic repression program. This indicates a mutual interference between DNA methylation and histone modification (Mohn et al., 2008; Schlesinger et al., 2007). Viré et al. discovered DNA methylation to be mechanistically linked to PcG proteins who normally influence gene activity by histone modification. EZH2 as part of the PRC2, controls CpG methylation by direct interaction with DNMT enzymatic activity. Even more, EZH2 was shown to be necessary for DNMT binding to target promotors (Viré et al.,

2006). Therefore, miR-203 is presumably down regulated by DNA methylation initially mediated via EZH2 repressive activity.

On the other hand, artificial up-regulation of miR-203 using a miRNA mimic revealed an influence on EZH2 expression. Very high miR-203 levels reduced EZH2 as well as EWS/FLI1 expression levels.

Obviously, there seems to be a feedback loop between miR-203 and EZH2 or EWS/FLI1. So far, in ES no specific deregulated miRNA was identified to influence EZH2. Several studies already demonstrated EZH2 to be the direct target of miR-124 or miR-101. Both investigations indicate a functional and mechanistic link between the tumor suppressor miRNAs and the oncogene EZH2 (Friedman et al., 2009; Zheng et al., 2012). Further studies are needed to address the question how miR-203 exactly influences EWS/FLI1 and EZH2 activity in ES. Thereby, subsequent investigations should also consider possible side effects. Unphysiological high levels of miR-203 that occurred after using the mimic could have influenced EWS/FLI1 and EZH2 in a still unknown way.

5.3.3 HDAC inhibition influences miR-203 expression level

HDACs induce gene inactivation by promoting inaccessible heterochromatin. TSA and MS-275 are HDAC inhibitors, whereby TSA works as a pan-HDAC inhibitor and MS-275 is more specific, inhibiting only class I HDACs (HDAC1, 2 and 3) and the class II A HDAC9 (Witt, Deubzer, Milde, & Oehme, 2009). Treating ES cells with both inhibitors led to a significantly increased expression of miR-203. This observation indicates a relationship between histone acetylation and histone methylation mediated by PRC2.

Several studies already reported a participation of HDAC activity in PRC2-mediated epigenetic gene silencing. Van der Vlag et al. found EED, one core component of the PRC2 complex to interact with HDACs, thus implementing its suppressive activity (van der Vlag, J & Otte, 1999). Even more, in prostate cancer EZH2-mediated gene silencing was highly dependent on HDAC activity. Here, treating prostate cancer cells with TSA completely reset the effects of EZH2 (Varambally et al., 2002). Similar results were obtained in ES (Richter et al., 2009) and in a study about aggressive breast cancer in which the overexpression of EZH2 in normal breast epithelial cells increased HDAC activity (Kleer et al., 2003).

Thus, miR-203 expression in ES is regulated by PRC2 depending on HDAC activity. Rephrased suppression of EZH2 by means of GSK126 resulted in an increased miR-203 expression and in a concurrent global increase of the “active” H3K9/14ac histone mark in western blot analysis. This again indicates the involvement of HDAC activity.

5.3.4 miR-203 biological effects

ES is an aggressively growing solid bone tumor that metastasizes soon to bone and lung tissues. To confirm the role of miR-203 as a tumor suppressor miRNA in ES several functional *in vitro* assays were performed. Therefore, ES cell lines were treated with a mimic for miR-203 and changes in biological characteristics were monitored. As a first observation, treated ES cells showed a decreased invasive capacity *in vitro.* In the next step anchorage independent growth was examined by performing colony formation assays using methylcellulose-based media. Cells exhibiting high miR-203 expression revealed a reduced ability to grow contact independently. Finally, the influence on contact-dependent proliferation capacity was examined. Whereby, the up-regulation of miR-203 also resulted in a lower proliferation rate. This overall indicates that miR-203 is able to inhibit tumor specific capacities.

Subsequently, to confirm the *in vitro* results their role in two different xenograft mouse models was analyzed. Therefore, ES cells with constitutive high miR-203 expression were generated and the effect on local tumor growth as well as on metastatic capacity was monitored. Unfortunately, none of the *in vivo* experiments was able to confirm the *in vitro* results. Neither a change of the metastatic behavior nor a delay of local tumor growth could be measured. Although, all tumor samples *ex vivo* still demonstrated high miR-203 expression levels there was no difference in survival between the two groups.

Considering the discrepancy between the promising *in vitro* and the down pointing *in vivo* results it is important to further elucidate the method of miRNA mimics. These chemically synthesized, double-stranded RNA molecules imitate endogenous miRNAs expression but at complete supraphysiological levels. The miRNA mimic used in this study reached values that were 250 000-fold higher than the reference. It can be supposed that there are still unknown side effects on biological processes caused by such very high expression levels. Subsequently, further experimental approaches with lower expression levels should be carried out.

Continuous advancement of synthetic miRNA mimics and antagomirs will contribute to avoid side effects and may approve *in vivo* results in the near future.

6. Summary

The Ewing sarcoma (ES) is the second most common malignancy of bone and soft tissue in children and adolescents. Pathological it manifests with poorly differentiated and highly malignant tumor cells of uncertain histogenesis and has a characteristic genetic background. The balanced chromosomal translocation between chromosomes 11 and 22 leads to an aberrant oncogene that influences gene expression and oncogenic transformation. The most common fusion combines the *EWS* gene and one gene of the *ETS* family: in 85% FLI1.

EWS/FLI1 regulates the expression of the histone methyltransferase EZH2 (enhancer of zeste, Drosophila, homolog 2), thereby employing epigenetic mechanisms to promote and maintain an undifferentiated and highly malignant phenotype of ES.

This thesis examined for the first time, microRNAs (miRNAs) to be part of those epigenetic regulation mechanisms. MiRNAs are endogenous small double-stranded non-protein coding RNA molecules that play a decisive role in post-transcriptional gene regulation processes in physiology and disease.

Gene expression analysis by qRT-PCR revealed miR-203 to be down regulated in ES. RNA-inference mediated EZH2 knock down as well as enzymatic inhibition by GSK126 resulted in reexpression of miR-203. Similarly, the histone deacetylase (HDAC) inhibitors TSA and MS-275 as well as the DNA methyltransferase (DNMT) inhibitor 5AzaC led to an increased miR-203 level. As artificial increased miR-203 expression inhibits tumor specific capacities like invasiveness and contact independent growth it must be considered as a tumor suppressor miRNA in ES downregulated by EZH2 and HDAC mediated DNA hypermethylation.

In contrast qRT-PCR analysis showed miR-497 to be up-regulated in ES. Thereby, EZH2 knock down as well as GSK126 treatment generated an attenuated expression of miR-497.

However, after the treatment with the HDAC inhibitors miR-497 expression increased again. This time, inhibition of miR-497 merely influenced the capacity of invasive growth. It seems, miR-497 has some oncogenic potential in ES maintained by EZH2 in a still not understood way.

Finally, miR-211 showed contrary to previous studies only intermediate expression levels in ES. Neither up-regulation using a mimic nor down-regulation with an inhibitor provided any significant results. Similarly, there were no relevant alterations on the epigenetic level. Therefore, miR-221 seems not to have a relevant impact on ES pathogenesis.

Taken together, this study shed further light into the relevance of three miRNAs for ES malignancy. These results and the thereof better understanding of basic genetic regulation processes may lead to new ES-specific targets for alternative target-orientated therapeutic strategies.

7. Zusammenfassung

Das Ewing Sarkom (ES) ist der zweithäufigste maligne Knochen- und Weichteiltumor des Kindes- und Jugendalters. Er zeichnet sich durch wenig differenzierte, äußerst bösartige Tumorzellen mit unklarem histologischem Ursprung und durch einen charakteristischen genetischen Hintergrund aus. Eine balancierte chromosomale Translokation zwischen den Chromosomen 11 und 22 führt zu einem Onkogen, das Genexpression und damit onkogene Transfomation beeinflusst. Das häufigste Fusionsgen kombiniert dabei Gene der EWS-Familie mit solchen der ETS-Familie (in 85% FLI1).

EWS-FLI1 reguliert die Expression der Histonmethyltransferase EZH2, wobei epigenetische Mechanismen begünstigt werden, die einen undifferenzierten und hochmalignen Phänotypen des ES unterhalten.

Diese Arbeit untersuchte zum ersten Mal microRNAs (miRNAs) als Teil dieser epigenetischen Regulationsmechanismen. miRNAs sind endogene, kleine, doppelsträngige, nicht-proteinkodierende RNA Moleküle, die eine entscheidende Rolle für posttranskriptionelle Genregulationsprozesse sowohl beim Gesunden als auch beim Kranken spielen.

Genexpressionsanalysen mit Hilfe von qRT-PCR konnten zeigen, dass miR-203 im ES herunter reguliert wird. Eine EZH2 Suppression, sowohl durch RNA-Interferenz also auch durch enzymatische Inhibierung mittels GSK-126 führte zu einer erneuten Expression von miR-203. In ähnlicher Weise führten die Histondeazetylase (HDAC) Inhibitoren TSA und MS-275 sowie der DNA-Mehyltransferase (DNMT) Inhibitor 5AzaC zu einem Wiederanstieg der miR-203 Expression. Nachdem eine artifiziell erhöhte miR-203 Expression tumorspezifische Fähigkeiten wie invasives und kontaktunabhängiges Wachstum behinderten, wurde in Betracht gezogen, dass miR-203 im ES als Tumor-Suppressor fungiert. Dabei scheint es, als würde miR-203 vor allem durch EZH2 und HDAC vermittelte DNA-Hypermethylierung supprimiert.

Im Gegensatz dazu, zeigten qRT-PCR Analysen, dass miR-497 im ES hoch reguliert wird, wobei die Expression nach EZH2 Suppression und GSK126 vermittelter Inhibierung abnahm. Sie stieg allerdings nach Behandlung mit HDAC Inhibitoren wieder an. In diesem Fall beeinflusste die Inhibition von miR-497 lediglich die Fähigkeit eines invasiven Wachstums. Es scheint, als habe miR-497 durchaus onkogenes Potential im ES, welches durch EZH2 auf noch unbekannte Weise aufrechterhalten wird.

Zu guter Letzt, zeigte miR-221 im Gegensatz zu vorherigen Studien lediglich ein intermediäres Expressionsniveau im ES. Weder eine Hochregulierung mit Hilfe einer Mimic, noch eine Suppression mit einem Inhibitor erbrachten signifikante Ergebnisse. In ähnlicher Weise zeigten sich auch keine relevanten Veränderungen auf epigenetischer Ebene. Es scheint, als habe miR-221 keinen relevanten Einfluss auf die Pathogenes des ES.

Zusammengenommen richtete diese Arbeit ein besonderes Augenmerk auf die Relevanz dreier miRNAs für die Malignität des ES. Die Ergebnisse und das daraus resultierende bessere Verständnis grundlegendster genetischer Regulationsprozesse mögen zu neuen ES-spezifischen Angriffspunkten für alternative zielorientierte therapeutische Strategien führen.

8. References

Agelopoulos, K., Richter, G., Schmidt, E., Dirksen, U., Heyking, K. von, Moser, B., Klein, H.-U., Kontny, U., Dugas, M., Poos, K., Korsching, E., Buch, T., Weckesser, M., Schulze, I., Besoke, R., Witten, A., Stoll, M., Kohler, G., Hartmann, W., Wardelmann, E., Rossig, C., Baumhoer, D., Jürgens, H., Burdach, S., Berdel, W. E., & Müller-Tidow, C. (2015). Deep Sequencing in Conjunction with Expression and Functional Analyses Reveals Activation of FGFR1 in Ewing Sarcoma. *Clinical Cancer Research: an official journal of the American Association for Cancer Research*, 4935–4946.

Ban, J., Jug, G., Mestdagh, P., Schwentner, R., Kauer, M., Aryee, D. N. T., Schaefer, K.-L., Nakatani, F., Scotlandi, K., Reiter, M., Strunk, D., Speleman, F., Vandesompele, J., & Kovar, H. (2011). Hsa-mir-145 is the top EWS-FLI1-repressed microRNA involved in a positive feedback loop in Ewing's sarcoma. *Oncogene*, 2173–2180.

Bartel, D. (2004). MicroRNAsGenomics, Biogenesis, Mechanism, and Function. *Cell*, 281–297.

Bernstein, M., Kovar, H., Paulussen, M., Randall, R. L., Schuck, A., Teot, L. A., & Juergens, H. (2006). Ewing's sarcoma family of tumors: current management. *The Oncologist*, 503–519.

Böcker, W., & Aguzzi, A. (2008). *Pathologie* (4., vollst. überarb. Aufl). München: Elsevier, Urban & Fischer.

Bueno, M. J., Pérez de Castro, I., Gómez de Cedrón, M., Santos, J., Calin, G. A., Cigudosa, J. C., Croce, C. M., Fernández-Piqueras, J., & Malumbres, M. (2008). Genetic and epigenetic silencing of microRNA-203 enhances ABL1 and BCR-ABL1 oncogene expression. *Cancer Cell*, 496–506.

Burchill, S. A. (2003). Ewing's sarcoma: diagnostic, prognostic, and therapeutic implications of molecular abnormalities. *Journal of Clinical Pathology*, 96–102.

Burdach, S., & Jürgens, H. (2002). High-dose chemoradiotherapy (HDC) in the Ewing family of tumors (EFT). *Critical Reviews in Oncology/Hematology*, 169–189.

Burdach, S., Plehm, S., Unland, R., Dirksen, U., Borkhardt, A., Staege, M. S., Müller-Tidow, C., & Richter, G. (2009). Epigenetic maintenance of stemness and malignancy in peripheral neuroectodermal tumors by EZH2. *Cell Cycle*, 1991–1996.

Cao, Q., Yu, J., Dhanasekaran, S. M., Kim, J. H., Mani, R.-S., Tomlins, S. A., Mehra, R., Laxman, B., Cao, X., Kleer, C. G., Varambally, S., & Chinnaiyan, A. M. (2008). Repression of E-cadherin by the polycomb group protein EZH2 in cancer. *Oncogene*, 7274–7284.

Christman, J. K. (2002). 5-Azacytidine and 5-aza-2'-deoxycytidine as inhibitors of DNA methylation: mechanistic studies and their implications for cancer therapy. *Oncogene*, 5483–5495.

Dhordain, P., Quief, S., Lantoine, D., Kerckaert, J.-P., Albagli, O., Lin, R. J., & Evans, R. M. (1998). The LAZ3 (BCL-6) oncoprotein recruits a SMRT/mSIN3A/histone deacetylase containing complex to mediate transcriptional repression. *Nucleic Acids Research*, 4645–4651.

Diao, Y., Guo, X., Jiang, L., Wang, G., Zhang, C., Wan, J., Jin, Y., & Wu, Z. (2014). miR-203, a tumor suppressor frequently down-regulated by promoter hypermethylation in rhabdomyosarcoma. *The Journal of Biological Chemistry*, 529–539.

Diederichs, S., & Haber, D. A. (2007). Dual role for argonautes in microRNA processing and posttranscriptional regulation of microRNA expression. *Cell*, 1097–1108.

Dobosy, J. R., & Selker, E. U. (2001). Emerging connections between DNA methylation and histone acetylation. *Cellular and Molecular Life Sciences*, 721–727.

Egger, G., Liang, G., Aparicio, A., & Jones, P. A. (2004). Epigenetics in human disease and prospects for epigenetic therapy. *Nature*, 457–463.

Esteller, M. (2002). CpG island hypermethylation and tumor suppressor genes: a booming present, a brighter future. *Oncogene*, 5427–5440.

Esteller, M. (2007). Cancer epigenomics: DNA methylomes and histone-modification maps. *Nature Reviews Genetics*, 286–298.

Ewing, J. (1972). Diffuse Endothelioma of Bone: Reprinted from the Proceedings of the New York Pathological Society 21: 17–24, 1921. *CA: A Cancer Journal for Clinicians*, 95–98.

Fabbri, M., Garzon, R., Cimmino, A., Liu, Z., Zanesi, N., Callegari, E., Liu, S., Alder, H., Costinean, S., Fernandez-Cymering, C., Volinia, S., Guler, G., Morrison, C. D., Chan, K. K., Marcucci, G., Calin, G. A., Huebner, K., & Croce, C. M. (2007). MicroRNA-29 family reverts aberrant methylation in lung cancer by targeting DNA methyltransferases 3A and 3B. *Proceedings of the National Academy of Sciences of the United States of America*, 15805–15810.

Fahrner, J. A., Eguchi, S., Herman, J. G., & Baylin, S. B. (2002). Dependence of histone modifications and gene expression on DNA hypermethylation in cancer. *Cancer Research*, 7213–7218.

Feng, B., & Chen, L. (2009). Review of mesenchymal stem cells and tumors: executioner or coconspirator? *Cancer Biotherapy & Radiopharmaceuticals*, 717–721.

Fenrick, R., & Hiebert, S. W. (1998). Role of histone deacetylases in acute leukemia. *Journal of Cellular Biochemistry. Supplement*, 194–202.

Filipowicz, W., Bhattacharyya, S. N., & Sonenberg, N. (2008). Mechanisms of post-transcriptional regulation by microRNAs: are the answers in sight? *Nature Reviews Genetics*, 102–114.

Fornari, F., Gramantieri, L., Ferracin, M., Veronese, A., Sabbioni, S., Calin, G. A., Grazi, G. L., Giovannini, C., Croce, C. M., Bolondi, L., & Negrini, M. (2008). MiR-221 controls CDKN1C/p57 and CDKN1B/p27 expression in human hepatocellular carcinoma. *Oncogene*, 5651–5661.

Frenquelli, M., Muzio, M., Scielzo, C., Fazi, C., Scarfò, L., Rossi, C., Ferrari, G., Ghia, P., & Caligaris-Cappio, F. (2010). MicroRNA and proliferation control in chronic lymphocytic leukemia: functional relationship between miR-221/222 cluster and p27. *Blood*, 3949–3959.

Friedman, J. M., Liang, G., Liu, C.-C., Wolff, E. M., Tsai, Y. C., Ye, W., Zhou, X., & Jones, P. A. (2009). The putative tumor suppressor microRNA-101 modulates the cancer epigenome by repressing the polycomb group protein EZH2. *Cancer Research*, 2623–2629.

Furuta, M., Kozaki, K., Tanaka, S., Arii, S., Imoto, I., & Inazawa, J. (2010). miR-124 and miR-203 are epigenetically silenced tumor-suppressive microRNAs in hepatocellular carcinoma. *Carcinogenesis*, 766–776.

Furuta, M., Kozaki, K., Tanimoto, K., Tanaka, S., Arii, S., Shimamura, T., Niida, A., Miyano, S., & Inazawa, J. (2013). The tumor-suppressive miR-497-195 cluster targets multiple cell-cycle regulators in hepatocellular carcinoma. *PloS one*, 1–12.

Galardi, S., Mercatelli, N., Giorda, E., Massalini, S., Frajese, G. V., Ciafrè, S. A., & Farace, M. G. (2007). miR-221 and miR-222 expression affects the proliferation potential of human prostate carcinoma cell lines by targeting p27Kip1. *The Journal of Biological Chemistry*, 23716–23724.

Garzon, R., Volinia, S., Liu, C.-G., Fernandez-Cymering, C., Palumbo, T., Pichiorri, F., Fabbri, M., Coombes, K., Alder, H., Nakamura, T., Flomenberg, N., Marcucci, G., Calin, G. A., Kornblau, S. M., Kantarjian, H., Bloomfield, C. D., Andreeff, M., & Croce, C. M. (2008). MicroRNA signatures associated with cytogenetics and prognosis in acute myeloid leukemia. *Blood*, 3183–3189.

Ge, L., Zheng, B., Li, M., Niu, L., & Li, Z. (2016). MicroRNA-497 suppresses osteosarcoma tumor growth in vitro and in vivo. *Oncology Letters*, 2207–2212.

Gee, H. E., Buffa, F. M., Camps, C., Ramachandran, A., Leek, R., Taylor, M., Patil, M., Sheldon, H., Betts, G., Homer, J., West, C., Ragoussis, J., & Harris, A. L. (2011). The small-nucleolar RNAs commonly used for microRNA normalisation correlate with tumour pathology and prognosis. *British journal of cancer*, 1168–1177.

Giard, D. J., Aaronson, S. A., Todaro, G. J., Arnstein, P., Kersey, J. H., Dosik, H., & Parks, W. P. (1973). In vitro cultivation of human tumors: establishment of cell lines derived from a series of solid tumors. *Journal of the National Cancer Institute*, 1417–1423.

Goldman, J. P., Blundell, M. P., Lopes, L., Kinnon, C., DI Santo, James P, & Thrasher, A. J. (1998). Enhanced human cell engraftment in mice deficient in RAG2 and the common cytokine receptor gamma chain. *British Journal of Haematology*, 335–342.

Gregory, R. I., Chendrimada, T. P., Cooch, N., & Shiekhattar, R. (2005). Human RISC couples microRNA biogenesis and posttranscriptional gene silencing. *Cell*, 631–640.

He, L., He, X., Lim, L. P., Stanchina, E. de, Xuan, Z., Liang, Y., Xue, W., Zender, L., Magnus, J., Ridzon, D., Jackson, A. L., Linsley, P. S., Chen, C., Lowe, S. W., Cleary, M. A., & Hannon, G. J. (2007). A microRNA component of the p53 tumour suppressor network. *Nature*, 1130–1134.

Hensel, T., Giorgi, C., Schmidt, O., Calzada-Wack, J., Neff, F., Buch, T., Niggli, F. K., Schafer, B. W., Burdach, S., & Richter, G. (2016). Targeting the EWS-ETS transcriptional program by BET bromodomain inhibition in Ewing sarcoma. *Oncotarget*, 1451–1463.

Herman, J. G., & Baylin, S. B. (2003). Gene silencing in cancer in association with promoter hypermethylation. *The New England Journal of Medicine*, 2042–2054.

Jedlicka, P. (2010). Ewing Sarcoma, an enigmatic malignancy of likely progenitor cell origin, driven by transcription factor oncogenic fusions. *International Journal of Clinical and Experimental Pathology*, 338–347.

Jenuwein, T., & Allis, C. D. (2001). Translating the histone code. *Science*, 1074–1080.

Jones, P. A., & Baylin, S. B. (2002). The fundamental role of epigenetic events in cancer. *Nature Reviews Genetics*, 415–428.

Kaatsch, P., & Spix, C. (2015). German Cancer Childhood Registry - Annual Report 2015 (1980-2014). *Institute of Medical Biostatistics, Epidemoilogie and Informatics (IMBEI) at the University Medical Center of the Johannes Gutenberg University, Mainz*, 52.

Ke, N., Wang, X., Xu, X., & Abassi, Y. (2011). The xCELLigence system for real-time and label-free monitoring of cell viability. *Methods in Molecular Biology*, 33–43.

Kedde, M., Strasser, M. J., Boldajipour, B., Oude Vrielink, J., Slanchev, K., Le Sage, C., Nagel, R., Voorhoeve, P. M., van Duijse, J., Ørom, U. A., Lund, A. H., Perrakis, A., Raz, E., & Agami, R. (2007). RNA-binding protein Dnd1 inhibits microRNA access to target mRNA. *Cell*, 1273–1286.

Kim, Y.-K., Yu, J., Han, T. S., Park, S.-Y., Namkoong, B., Kim, D. H., Hur, K., Yoo, M.-W., Lee, H.-J., Yang, H.-K., & Kim, V. N. (2009). Functional links between clustered microRNAs: suppression of cell-cycle inhibitors by microRNA clusters in gastric cancer. *Nucleic Acids Research*, 1672–1681.

Kleer, C. G., Cao, Q., Varambally, S., Shen, R., Ota, I., Tomlins, S. A., Ghosh, D., Sewalt, Richard G A B, Otte, A. P., Hayes, D. F., Sabel, M. S., Livant, D., Weiss, S. J., Rubin, M. A., & Chinnaiyan, A. M. (2003). EZH2 is a marker of aggressive breast cancer and promotes neoplastic transformation of breast epithelial cells. *Proceedings of the National Academy of Sciences of the United States of America*, 11606–11611.

Kozaki, K., Imoto, I., Mogi, S., Omura, K., & Inazawa, J. (2008). Exploration of tumor-suppressive microRNAs silenced by DNA hypermethylation in oral cancer. *Cancer Research*, 2094–2105.

Lahl, M., Fisher, V. L., & Laschinger, K. (2008). Ewing's sarcoma family of tumors: an overview from diagnosis to survivorship. *Clinical Journal of Oncology Nursing*, 89–97.

Lawrence, M. S., Stojanov, P., Polak, P., Kryukov, G. V., Cibulskis, K., Sivachenko, A., Carter, S. L., Stewart, C., Mermel, C. H., Roberts, S. A., Kiezun, A., Hammerman, P. S., McKenna, A., Drier, Y., Zou, L., Ramos, A. H., Pugh, T. J., Stransky, N., Helman, E., Kim, J., Sougnez, C., Ambrogio, L., Nickerson, E., Shefler, E., Cortes, M. L., Auclair, D., Saksena, G., Voet, D., Noble, M., DiCara, D., Lin, P., Lichtenstein, L., Heiman, D. I., Fennell, T., Imielinski, M.,

Hernandez, B., Hodis, E., Baca, S., Dulak, A. M., Lohr, J., Landau, D.-A., Wu, C. J., Melendez-Zajgla, J., Hidalgo-Miranda, A., Koren, A., McCarroll, S. A., Mora, J., Lee, R. S., Crompton, B., Onofrio, R., Parkin, M., Winckler, W., Ardlie, K., Gabriel, S. B., Roberts, C. W. M., Biegel, J. A., Stegmaier, K., Bass, A. J., Garraway, L. A., Meyerson, M., Golub, T. R., Gordenin, D. A., Sunyaev, S., Lander, E. S., & Getz, G. (2013). Mutational heterogeneity in cancer and the search for new cancer-associated genes. *Nature*, 214–218.

Lessnick, S., & Ladanyi, M. (2012). Molecular pathogenesis of Ewing sarcoma: new therapeutic and transcriptional targets. *Annual Review of Pathology*, 145–159.

Li, D., Zhao, Y., Liu, C., Chen, X., Qi, Y., Jiang, Y., Zou, C., Zhang, X., Liu, S., Wang, X., Zhao, D., Sun, Q., Zeng, Z., Dress, A., Lin, M. C., Kung, H.-F., Rui, H., Liu, L.-Z., Mao, F., Jiang, B.-H., & Lai, L. (2011). Analysis of MiR-195 and MiR-497 expression, regulation and role in breast cancer. *Clinical Cancer Research: an official journal of the American Association for Cancer Research*, 1722–1730.

Li, S., Peters, G. A., Ding, K., Zhang, X., Qin, J., & Sen, G. C. (2006). Molecular basis for PKR activation by PACT or dsRNA. *Proceedings of the National Academy of Sciences of the United States of America*, 10005–10010.

Lu, J., Getz, G., Miska, E. A., Alvarez-Saavedra, E., Lamb, J., Peck, D., Sweet-Cordero, A., Ebert, B. L., Mak, R. H., Ferrando, A. A., Downing, J. R., Jacks, T., Horvitz, H. R., & Golub, T. R. (2005). MicroRNA expression profiles classify human cancers. *Nature*, 834–838.

Lujambio, A., Calin, G. A., Villanueva, A., Ropero, S., Sánchez-Céspedes, M., Blanco, D., Montuenga, L. M., Rossi, S., Nicoloso, M. S., Faller, W. J., Gallagher, W. M., Eccles, S. A., Croce, C. M., & Esteller, M. (2008). A microRNA DNA methylation signature for human cancer metastasis. *Proceedings of the National Academy of Sciences of the United States of America*, 13556–13561.

Mattick, J. S., & Makunin, I. V. (2005). Small regulatory RNAs in mammals. *Human Molecular Genetics*, R121-R132.

McKinsey, E., Parrish, J. K., Irwin, A. E., Niemeyer, B. F., Kern, H. B., Birks, D. K., & Jedlicka, P. (2011). A novel oncogenic mechanism in Ewing sarcoma involving IGF pathway targeting by EWS/Fli1-regulated microRNAs. *Oncogene*, 4910–4920.

Meister, G. (2013). Argonaute proteins: functional insights and emerging roles. *Nature Reviews Genetics*, 447–459.

Mercatelli, N., Coppola, V., Bonci, D., Miele, F., Costantini, A., Guadagnoli, M., Bonanno, E., Muto, G., Frajese, G. V., Maria, R. de, Spagnoli, L. G., Farace, M. G., & Ciafrè, S. A. (2008). The inhibition of the highly expressed miR-221 and miR-222 impairs the growth of prostate carcinoma xenografts in mice. *PloS one*, 1–10.

Mogilyansky, E., & Rigoutsos, I. (2013). The miR-17/92 cluster: a comprehensive update on its genomics, genetics, functions and increasingly important and numerous roles in health and disease. *Cell Death and Differentiation*, 1603–1614.

Mohn, F., Weber, M., Rebhan, M., Roloff, T. C., Richter, J., Stadler, M. B., Bibel, M., & Schübeler, D. (2008). Lineage-specific polycomb targets and de novo DNA methylation define restriction and potential of neuronal progenitors. *Molecular Cell*, 755–766.

Moosmann, S., Hutter, J., Moser, C., Krombach, F., & Huss, R. (2005). Milieu-adopted in vitro and in vivo differentiation of mesenchymal tissues derived from different adult human CD34-negative progenitor cell clones. *Cells Tissues Organs*, 91–101.

Nassirpour, R., Mehta, P. P., Baxi, S. M., & Yin, M.-J. (2013). miR-221 promotes tumorigenesis in human triple negative breast cancer cells. *PloS one*, 1–9.

Noonan, E. J., Place, R. F., Pookot, D., Basak, S., Whitson, J. M., Hirata, H., Giardina, C., & Dahiya, R. (2009). miR-449a targets HDAC-1 and induces growth arrest in prostate cancer. *Oncogene*, 1714–1724.

O'Donnell, K. A., Wentzel, E. A., Zeller, K. I., Dang, C. V., & Mendell, J. T. (2005). c-Myc-regulated microRNAs modulate E2F1 expression. *Nature*, 839–843.

Park, J.-K., Lee, E. J., Esau, C., & Schmittgen, T. D. (2009). Antisense inhibition of microRNA-21 or -221 arrests cell cycle, induces apoptosis, and sensitizes the effects of gemcitabine in pancreatic adenocarcinoma. *Pancreas*, 1–9.

Peltier, H. J., & Latham, G. J. (2008). Normalization of microRNA expression levels in quantitative RT-PCR assays: identification of suitable reference RNA targets in normal and cancerous human solid tissues. *RNA*, 844–852.

Pineau, P., Volinia, S., McJunkin, K., Marchio, A., Battiston, C., Terris, B., Mazzaferro, V., Lowe, S. W., Croce, C. M., & Dejean, A. (2010). miR-221 overexpression contributes to liver tumorigenesis. *Proceedings of the National Academy of Sciences of the United States of America*, 264–269.

Pinto, A., Dickman, P., & Parham, D. (2011). Pathobiologic markers of the ewing sarcoma family of tumors: state of the art and prediction of behaviour. *Sarcoma*, 1–15.

Plehm, S. (2011). Epigenetic regulation of stemness and malignancy in Ewing Tumors. Technische Universität, München.

Richter, G., Plehm, S., Fasan, A., Rössler, S., Unland, R., Bennani-Baiti, I. M., Hotfilder, M., Löwel, D., Luettichau, I. von, Mossbrugger, I., Quintanilla-Martinez, L., Kovar, H., Staege, M. S., Müller-Tidow, C., & Burdach, S. (2009). EZH2 is a mediator of EWS/FLI1 driven tumor growth and metastasis blocking endothelial and neuro-ectodermal differentiation. *Proceedings of the National Academy of Sciences of the United States of America*, 5324–5329.

Riggi, N., Knoechel, B., Gillespie, S. M., Rheinbay, E., Boulay, G., Suvà, M.-L., Rossetti, N. E., Boonseng, W. E., Oksuz, O., Cook, E. B., Formey, A., Patel, A., Gymrek, M., Thapar, V., Deshpande, V., Ting, D. T., Hornicek, F. J., Nielsen, G. P., Stamenkovic, I., Aryee, M. J., Bernstein, B. E., & Rivera, M. N. (2014). EWS-FLI1 utilizes divergent chromatin remodeling mechanisms to directly activate or repress enhancer elements in Ewing sarcoma. *Cancer Cell*, 668–681.

Riggi, N., Suvà, M.-L., & Stamenkovic, I. (2009). Ewing's sarcoma origin: from duel to duality. *Expert Review of Anticancer Therapy*, 1025–1030.

Riggi, N., Cironi, L., Provero, P., Suvà, M.-L., Kaloulis, K., Garcia-Echeverria, C., Hoffmann, F., Trumpp, A., & Stamenkovic, I. (2005). Development of Ewing's sarcoma from primary bone marrow-derived mesenchymal progenitor cells. *Cancer Research*, 11459–11468.

Riggi, N., Suvà, M.-L., Vito, C. de, Provero, P., Stehle, J.-C., Baumer, K., Cironi, L., Janiszewska, M., Petricevic, T., Suvà, D., Tercier, S., Joseph, J.-M., Guillou, L., & Stamenkovic, I. (2010). EWS-FLI-1 modulates miRNA145 and SOX2 expression to initiate mesenchymal stem cell reprogramming toward Ewing sarcoma cancer stem cells. *Genes & Development*, 916–932.

Robin, T. P., Smith, A., McKinsey, E., Reaves, L., Jedlicka, P., & Ford, H. L. (2012). EWS/FLI1 regulates EYA3 in Ewing sarcoma via modulation of miRNA-708, resulting in increased cell survival and chemoresistance. *Molecular Cancer Research*, 1098–1108.

Saini, S., Majid, S., Yamamura, S., Tabatabai, L., Suh, S. O., Shahryari, V., Chen, Y., Deng, G., Tanaka, Y., & Dahiya, R. (2011). Regulatory Role of mir-203 in Prostate Cancer Progression

and Metastasis. *Clinical Cancer Research: an official journal of the American Association for Cancer Research*, 5287–5298.

Sankar, S., Bell, R., Stephens, B., Zhuo, R., Sharma, S., Bearss, D. J., & Lessnick, S. (2013). Mechanism and relevance of EWS/FLI-mediated transcriptional repression in Ewing sarcoma. *Oncogene*, 5089–5100.

Schlesinger, Y., Straussman, R., Keshet, I., Farkash, S., Hecht, M., Zimmerman, J., Eden, E., Yakhini, Z., Ben-Shushan, E., Reubinoff, B. E., Bergman, Y., Simon, I., & Cedar, H. (2007). Polycomb-mediated methylation on Lys27 of histone H3 pre-marks genes for de novo methylation in cancer. *Nature Genetics*, 232–236.

Schübeler, D., MacAlpine, D. M., Scalzo, D., Wirbelauer, C., Kooperberg, C., van Leeuwen, F., Gottschling, D. E., O'Neill, L. P., Turner, B. M., Delrow, J., Bell, S. P., & Groudine, M. (2004). The histone modification pattern of active genes revealed through genome-wide chromatin analysis of a higher eukaryote. *Genes & Development*, 1263–1271.

Schwarz, D. S., Hutvágner, G., Du, T., Xu, Z., Aronin, N., & Zamore, P. D. (2003). Asymmetry in the Assembly of the RNAi Enzyme Complex. *Cell*, 199–208.

Shen, L., Li, J., Xu, L., Ma, J., Li, H., Xiao, X., Zhao, J., & Fang, L. (2012). miR-497 induces apoptosis of breast cancer cells by targeting Bcl-w. *Experimental and therapeutic medicine*, 475–480.

Shu, S., & Polyak, K. (2017). BET Bromodomain Proteins as Cancer Therapeutic Targets. *Cold Spring Harbor Symposia on Quantitative Biology*, 1–7.

Staege, M. S., Hutter, C., Neumann, I., Foja, S., Hattenhorst, U. E., Hansen, G., Afar, D., & Burdach, S. (2004). DNA microarrays reveal relationship of Ewing family tumors to both endothelial and fetal neural crest-derived cells and define novel targets. *Cancer Research*, 8213–8221.

Stenvang, J., Petri, A., Lindow, M., Obad, S., & Kauppinen, S. (2012). Inhibition of microRNA function by antimiR oligonucleotides. *Silence*, 1–17.

Stinson, S., Lackner, M. R., Adai, A., Yu, N., Kim, H.-J., O'Brien, C., Spoerke, J., Jhunjhunwala, S., Boyd, Z., Januario, T., Newman, R. J., Yue, P., Bourgon, R., Modrusan, Z., Stern, H. M., Warming, S., de Sauvage, Frederic J, Amler, L., Yeh, R.-F., & Dornan, D. (2011). miR-221/222 targeting of trichorhinophalangeal 1 (TRPS1) promotes epithelial-to-mesenchymal transition in breast cancer. *Science Signaling*, 1–5.

Strahl, B. D., & Allis, C. D. (2000). The language of covalent histone modifications. *Nature*, 41–45.

Suzuki, H., Takatsuka, S., Akashi, H., Yamamoto, E., Nojima, M., Maruyama, R., Kai, M., Yamano, H.-O., Sasaki, Y., Tokino, T., Shinomura, Y., Imai, K., & Toyota, M. (2011). Genome-wide profiling of chromatin signatures reveals epigenetic regulation of MicroRNA genes in colorectal cancer. *Cancer Research*, 5646–5658.

Tirode, F., Laud-Duval, K., Prieur, A., Delorme, B., Charbord, P., & Delattre, O. (2007). Mesenchymal stem cell features of Ewing tumors. *Cancer Cell*, 421–429.

Triché, T. J. (2008). Non-coding RNA in the Pathogenesis of Childhood Cancer. *SIOP Education Book*, 85–91.

Turner, B. M. (2002). Cellular Memory and the Histone Code. *Cell*, 285–291.

Van der Vlag, J, & Otte, A. P. (1999). Transcriptional repression mediated by the human polycomb-group protein EED involves histone deacetylation. *Nature Genetics*, 474–478.

Varambally, S., Dhanasekaran, S. M., Zhou, M., Barrette, T. R., Kumar-Sinha, C., Sanda, M. G., Ghosh, D., Pienta, K. J., Sewalt, Richard G A B, Otte, A. P., Rubin, M. A., & Chinnaiyan, A. M. (2002). The polycomb group protein EZH2 is involved in progression of prostate cancer. *Nature*, 624–629.

Vasudevan, S., & Steitz, J. A. (2007). AU-rich-element-mediated upregulation of translation by FXR1 and Argonaute 2. *Cell*, 1105–1118.

Viré, E., Brenner, C., Deplus, R., Blanchon, L., Fraga, M., Didelot, C., Morey, L., van Eynde, A., Bernard, D., Vanderwinden, J.-M., Bollen, M., Esteller, M., Di Croce, L., Launoit, Y. de, & Fuks, F. (2006). The Polycomb group protein EZH2 directly controls DNA methylation. *Nature*, 871–874.

Visone, R., Russo, L., Pallante, P., Martino, I. de, Ferraro, A., Leone, V., Borbone, E., Petrocca, F., Alder, H., Croce, C. M., & Fusco, A. (2007). MicroRNAs (miR)-221 and miR-222, both overexpressed in human thyroid papillary carcinomas, regulate p27Kip1 protein levels and cell cycle. *Endocrine-Related Cancer*, 791–798.

Vito, C. de, Riggi, N., Cornaz, S., Suvà, M.-L., Baumer, K., Provero, P., & Stamenkovic, I. (2012). A TARBP2-dependent miRNA expression profile underlies cancer stem cell properties and provides candidate therapeutic reagents in Ewing sarcoma. *Cancer Cell*, 807–821.

Winter, J., Jung, S., Keller, S., Gregory, R. I., & Diederichs, S. (2009). Many roads to maturity: microRNA biogenesis pathways and their regulation. *Nature Cell Biology*, 228–234.

Witt, O., Deubzer, H. E., Milde, T., & Oehme, I. (2009). HDAC family: What are the cancer relevant targets? *Cancer Letters*, 8–21.

Yang, D., Liu, G., & Wang, K. (2015). miR-203 Acts as a Tumor Suppressor Gene in Osteosarcoma by Regulating RAB22A. *PloS one*, 1–9.

Yang, W., Chendrimada, T. P., Wang, Q., Higuchi, M., Seeburg, P. H., Shiekhattar, R., & Nishikura, K. (2006). Modulation of microRNA processing and expression through RNA editing by ADAR deaminases. *Nature Structural & Molecular Biology*, 13–21.

Yang, X., Karuturi, M., Sun, F., Aau, M., Yu, K., Shao, R., Miller, L. D., Tan, Patrick Boon Ooi, & Yu, Q. (2009). CDKN1C (p57) is a direct target of EZH2 and suppressed by multiple epigenetic mechanisms in breast cancer cells. *PloS one*, 1–11.

Zhang, L., Huang, J., Yang, N., Greshock, J., Megraw, M. S., Giannakakis, A., Liang, S., Naylor, T. L., Barchetti, A., Ward, M. R., Yao, G., Medina, A., O'brien-Jenkins, A., Katsaros, D., Hatzigeorgiou, A., Gimotty, P. A., Weber, B. L., & Coukos, G. (2006). microRNAs exhibit high frequency genomic alterations in human cancer. *Proceedings of the National Academy of Sciences of the United States of America*, 9136–9141.

Zhang, Z., Zhang, B., Li, W., Fu, L., Zhu, Z., & Dong, J.-T. (2011). Epigenetic Silencing of miR-203 Upregulates SNAI2 and Contributes to the Invasiveness of Malignant Breast Cancer Cells. *Genes & Cancer*, 782–791.

Zheng, F., Liao, Y.-J., Cai, M.-Y., Liu, Y.-H., Liu, T.-H., Chen, S.-P., Bian, X.-W., Guan, X.-Y., Lin, M. C., Zeng, Y.-X., Kung, H.-F., & Xie, D. (2012). The putative tumour suppressor microRNA-124 modulates hepatocellular carcinoma cell aggressiveness by repressing ROCK2 and EZH2. *Gut*, 278–289.

9. Appendices

9.1 List of figures

9.2 List of tables

10. Acknowledgements

An dieser Stelle möchte ich mich bei allen bedanken, die zum Gelingen dieser Doktorarbeit beigetragen haben.
Mein besonderer Dank gilt:

Herrn Prof. Dr. Stefan Burdach und Herrn PD Dr. Günther Richter für die Aufnahme in die Arbeitsgruppe, die Bereitstellung dieses interessanten Themas sowie für die Begleitung und die Korrektur meiner Arbeit.

Tim Hensel für die Übernahme meiner Betreuung, die Einarbeitung in die experimentellen Grundlagen und die fortwährende Unterstützung bis zu Letzt.

Bedanken möchte ich mich natürlich auch bei allen anderen Mitarbeitern des Forschungszentrums für krebskranke Kinder für die Anregungen, die gute Zusammenarbeit, die gegenseitige Hilfestellung und natürlich für eine sehr schöne Zeit im Labor.

Und zu guter Letzt danke ich meinen Eltern für ihr entgegengebrachtes Vertrauen, die uneingeschränkte Unterstützung meines Werdegangs und das rege Interesse am Fortgang der Arbeit.